POLITECNICO DI MILANO

School of Industrial and Information Engineering
Master of Science in Biomedical Engineering

CONDITIONING OF A CAPACITIVE SENSOR FOR DETECTION OF TOLUENE IN EXHALED BREATH

Supervisor: Pietro Cerveri
Co-Supervisor: Davide Marzorati

Thesis of:
Alessia Celli
Student ID: 904822

Academic Year 2019-2020

Abstract

Lung cancer is one of the leading causes of cancer death worldwide. It is an heterogeneous disease, that may arise in many different clinical pathological patterns.
Usually, symptoms appear only at advanced stages (III or IV), thus diagnosis often occurs when the disease is more difficult to treat and this leads to poor prognosis and high mortality. In order to reduce cancer-related death, diagnosis of any malignancy must be performed as soon as possible: **early detection of lung cancer** is of relevant importance, since it would allow to avoid metastatic spread and consequently increase the possibility of successful treatment, leading to higher survival rates. This is the reason why many studies have been focusing on this purpose for more than forty years.
Secondary prevention is very important: there is a need for new techniques for **screening of high-risk population**, prior entering the clinical pipeline. Currently, various different approaches are applied for lung cancer screening purposes, particularly imaging techniques. The most commonly adopted screening method is 'Low-Dose Computed Tomography' (LCDT), but it often leads to overdiagnosis (i.e., high number of false positives).
In this scene, **Exhaled Breath Analysis**, concerning the study of the **Volatile Organic Compounds** (VOCs) that are present in the air exhaled by the lungs, has gained more and more attention, thanks to its potentiality to obtain, in a non-invasive manner, biomarkers that could aid in establishing the diagnosis of various pulmonary diseases. A lot of studies examine the use of very expensive and complex laboratory instruments, such as 'Gas Chromatography' (GC) and 'Mass Spectrometry' (MS), but more recent developments are focusing on the use of small portable devices able to perform real-time analysis of the VOCs present in the exhaled breath, called **'Electronic Noses'** (eNoses). Currently, it is reported that eNoses are able to discriminate between healthy and lung cancer patients, based on the analysis of the exhaled VOCs pattern, the so called 'breathprint'.
The aim of this work was to develop a **capacitive sensor system** able to measure the concentration of a specific VOC, that is **Toluene**, present in a gas mixure in a closed environment and in static conditions, with the expectation to be a starting point for future research targeting the application to exhaled breath samples.
This work has been accomplished by combining a polymer-based capacitive sensor with a readout electronic circuit based entirely on PSoC ('Programmable System on Chip'), a platform that includes many peripherals as well as a microcontroller on a single chip. In particular, the capacitive sensor has been assembled by using golden planar circular **interdigitated micro-electrode array** and, in the role of molecular recognition element, a thin-film **Toluene-imprinted polymer**, coupled to the electrode in a way that the sensor electrical capacitance is expected to vary in relation to the presence of the target Toluene molecule in a gas mixture.
The sensor, together with a basic PCB ('Printed Circuit Board') designed with 'Autodesk Eagle' for interfacing with the readout electronics has been mounted on a customized plastic

support, realized by 3D printing technique.
The firmware loaded onto the PSoC memory, that has been written using 'PSoC Creator', performs a capacitance-to-frequency conversion, producing a square wave whose frequency is dependent on the external sensor capacitance, and consequently measures the frequency in order to compute the capacitance value and send it via serial communication to the Graphical User Interface for data visualization.
The PSoC-based capacitive measurement system has been tested to several ceramic capacitors in the pico-Farad range, and its performance was compared to the one of the commercial FDC1004Q Capacitance-to-Digital Converter supplied by 'Texas Instruments', showing an acceptable accuracy in the range from 10 to 100 pF.
After the initial calibration tests, the proposed measurement system has been used to monitor the capacitance changes of the aforementioned polymer-based sensor, while performing a series of adsorption steps, during which the sensor and its support were closed, for time intervals of increasing duration, inside a glass chamber saturated with Toluene.
By comparing the developed PSoC-based sensing system with the miniaturized commercial Capacitance-to-Digital Converter, it showed satisfying accuracy within the range from 10 to 100 pF, even though not being constant all over the range. In fact, the percentage accuracy error, with respect to the reference value provided by the commercial device, tends to be higher close to the bottom of the measuring range, with a maximum percentage error of -9.83%, but to extremely low -0.10% error for the 100 pF capacitors.
The work presented in this manuscript represents only the first step in the path for developing new instrument for the detection of lung cancer at early stages and widespread population screening.

Sommario

Attualmente, il **cancro ai polmoni** è fra le principali cause di decessi oncologici in tutto il mondo. Si tratta di una malattia molto eterogenea, che puó manifestarsi in svariate forme patologiche. Purtroppo, esso viene spesso diagnosticato negli stadi piú avanzati (III e IV), quando le terapie attualmente in uso si rivelano meno efficaci, e ció è inevitabilmente associato ad una minore aspettativa di vita. Allo scopo di ridurre l'elevato tasso di mortalitá legato a questa malattia, la diagnosi dovrebbe essere effettuata il prima possibile, in maniera tale da evitare il diffondersi di metastasi in altri organi. La **diagnosi precoce** del cancro ai polmoni è dunque di importanza rilevante, in quanto aumenterebbe la possibilitá di successo dei trattamenti, portando di conseguenza ad un aumento del tasso di sopravvivenza. Da qui nasce la necessitá di ideare nuove tecniche di screening per attuare un controllo preventivo della popolazione ad alto rischio (la cosiddetta 'prevenzione secondaria'), allo scopo di valutare se un individuo debba o meno essere immesso nell'iter clinico previsto per diagnosticare in maniera definitiva la presenza di una neoplasia. Per tale ragione, numerosi studi negli ultimi anni si sono mossi verso questo obiettivo.
Allo stato attuale, svariate combinazioni di tecniche vengono usate con lo scopo di controllare la popolazione considerata ad alto rischio, in particolare tecniche di imaging come la 'Tomografia Computerizzata volumetrica polmonare a Bassa Dose' (in inglese LDCT, ovvero 'LowDose Computed Tomography'), ma essa, oltre ad essere comunque invasiva, produce un elevato numero di falsi positivi.
In questo scenario, l'**Analisi del Respiro Esalato**, ossia lo studio dei **Composti Volatili Organici** (VOCs) presenti nell'aria che viene espirata, ha ottenuto sempre maggiore attenzione, grazie alla potenzialitá di ottenere dei bio-marcatori, ovvero indicatori della presenza della malattia, in maniera assolutamente non invasiva.
Fra le varie tecnologie che sono state sviluppate a tal proposito, le piú comunemente utilizzate sono la 'Gascromatografia' (GC) e la 'Spettrometria di massa' (MS), le quali permettono di individuate i VOCs con elevata accuratezza, ma sono al contempo costose e complesse. Meritano particolare attenzione i sistemi basati su array di sensori, i cosiddetti **'Nasi Elettronici'** (eNoses): si tratta di dispositivi relativamente piccoli, portabili, in grado di effettuare l'analisi del respiro, in taluni casi anche in tempo reale, andando ad individuare dei pattern caratteristici presenti nei gas espirati dai pazienti (le cosiddette 'breathprint', ovver le 'impronte del respiro').
L'obiettivo ultimo di questo lavoro di tesi magistrale, era quello di sviluppare un **sistema basato su sensore capacitivo** che fosse in grado di misurare, con accuratezza e sufficiente selettivitá, la concentrazione di un determinato composto volatile organico, in questo caso il **Toluene**, presente in una miscela gassosa in ambiente chiuso e condizioni statiche, in maniera tale da essere applicabile in futuro ai campioni di aria esalata. Questo obiettivo è stato perseguito utilizzando sensore polimerico di capacitá, unitamente ad un circuito elettronico di lettura realizzatto esclusivamente per mezzo del PSoC ('Psogrammable System on

Chip'), una piattaforma che include varie periferiche ed un microcontrollore su di un singolo chip. Nel dettaglio, il suddetto sensore capacitivo è stato assemblato utilizzando un **array di microelettrodi interdigitati** in oro, dalla struttura planare e circolare, unito ad un sottile strato di **polimero imprintato con il Toluene**, l'elemento sensibile finalizzato al riconoscimento molecolare, accoppiato all'elettrodo in maniera tale da esibire una variazione della capacitá elettrica complessiva del sensore in relazione alla presenza del composto target (il Toluene) in un miscuglio gassoso.
Il sensore, assieme ad una semplice PCB ('Printed Circuit Board') realizzata per permetterne l'interfacciamento con il circuito di lettura, è stato montato su di un supporto in PLA realizzato mediante stampa 3D.
Il firmware caricato nella memoria PSoC, scritto utilizzando 'PSoC Creator', esegue una conversione capacitá-frequenza, producendo al suo interno una forma d'onda quadra la cui frequenza dipende dalla capacitá del sensore esterno: di conseguenza, il sistema va a misurare continuamente la frequenza dell'onda quadra generata, da essa ricava il valore di capacitá, per poi inviarlo tramite interfaccia seriale alla GUI ('Graphical User Interface') per una piú agevole visualizzazione.
Il sistema di misura capacitiva basato sul PSoC quivi proposto è stato innanzitutto testato su di una serie di condensatori ceramici nel range dei pico-Farad, ed i risultati ottenuti sono stati confrontati con un convertitore digitale di capacitá disponibile in commercio, FDC1004Q prodotto dalla 'Texas Instruments', ed hanno mostrato un'accuratezza sufficiente in un range dai 10 ai 100 pF.
Dopo i test iniziali di calibrazione, il sistema è stato utilizzato per monitorare le variazioni di capacitá nel suddetto sensore polimerico, mediante una serie di sessioni di assorbimento durante le queli il sensore montato sul suo supporto è stato mantenuto, per intervalli temporali di crescente durata, chiuso dentro una camera di vetro satura di Toluene gassoso.

Nel confronto con il convertitore commerciale integrato di capacitá, il sistema di misura capacitivo basato su PSoC quivi proposto ha mostrato di saper raggiungere valori di accuratezza soddisfacenti, nel range [10;100pF], sebbene l'errore non sia costante lungo tutto il range di misura. Infatti, l'errore di accuratezza, espresso in percentuale rispetto al riferimento fornito dal sensore commerciale, tedne ad essere peggiore nella parte piú bassa del range di misura, con valori fino a -9.83%, quando applicato a condensatori intorno ai 10 pF, mentre migliora notevolmente se testato su condensatori intorno ai 100 pF, con un errore percentuale di -0.10%.
Il lavoro presentato nel seguente elaborato costituisce il passo iniziale di un percorso ben piú lungo finalizzato allo sviluppo di nuova strumentazione applicabile per la diagnosi precoce del cancro ai polmoni o per un protocollo di screening della popolazione ad alto rischio.

Contents

List of Figures

List of Tables

List of abbreviations

VOCs	Volatile Organic Compounds
EBC	Exhaled Breath Condensate
MIP	Molecularly-Imprinted Polymer
NIP	Non-Imprinted Polymer
IDA	Inter-Digitated electrode Array
I.C.	Integrated Circuit
PSoC	Programmable System on Chip
PCB	Printed Circuit Board
CAD	Computer-Aided Design
PLA	Polylactic Acid
COPD	Chronic Obstructive Pulmonary Disease
SCLC	Small Cell Lung Cancer
NSCLC	Non-Small Cell Lung Cancer
LDCT	Low-Dose Computed Tomography
GUI	Graphical User Interface
IDE	Integrated Design Environment
GC	Gas Chromatography
MS	Mass Spectrometry
IMS	Ion Mobility Spectrometry
eNoses	Electronic Noses
SAW	Surface Acoustic Waves
QMB	Quartz MicroBalance MOS Metal Oxide Sensors
AI	Artificial Intelligence
PPB	Parts Per Billions

PPM	Parts Per Millions
SPS	Samples Per Second
ISR	Interrupt Service Routine
CCO	Capacitance-Controlled Oscillator
ADC	Analog-to-Digital Converter
UART	Universal Asynchronous Receiver Transmitter
DMA	Direct Memory Access
IDAC	Current Digital-to-Analog Converter

Chapter 1

Introduction

Lung cancer, one of the leading causes of cancer death worldwide, is an heterogeneous disease, that may arise in many different clinical pathological patterns: the 'World Health Organization' classification recognizes 20 different types of malignant lung neoplasms. The two main categories of lung cancer are:

- Small Cell Lung Cancer (SCLC), that accounts for 15% of cases.
- Non-Small Cell Lung Cancer (NSCLC), which accounts fro 85% of cases.
  NSCLC can be further classified into three major histological subtypes:
  - Adenocarcinoma;
  - Squamous Cell Carcinoma;
  - Large Cell Carcinoma.

Usually, symptoms appear only at advanced stages (III or IV), thus diagnosis often occurs when the disease is more difficult to treat and associated with lower possibility of survival, leading to higher mortality rates. In order to reduce cancer-related death, diagnosis of any malignancy must be performed as soon as possible: early detection of lung cancer is of relevant importance, since it would allow to avoid metastatic spread and consequently increase the possibility of successful treatment, leading to higher survival rates. This is the reason why many studies have been focusing on this purpose for the past forty years. Detection of lung cancer at early stages is challenging, because most of lung cancer patients either do not show any symptoms, or those signs are not easily distinguished from the ones of other pulmonary diseases [2] or from the ones due to aging: cough, dyspnea (i.e., shortness of breath), chest pain, fatigue, weight loss, and so on [3].

Diagnosis tools The gold standard for diagnosis of thoracic cancers is a biopsy indicating malignant cells, but it is a very invasive procedure. Furthermore, in some situations, such as in severe COPD (Chronic Obstructive Pulmonary Disease) patients, it is not possible to extract enough tissue, thus diagnosis can only be established by a multidisciplinary team based on radiology combined with clinical data [4]. Usually, high-risk subjects who are suspected to have lung cancer undergo screening procedures with the aim of detecting the disease at the beginning of its development. Those screening tests should try to be as non-invasive as possible for the population, since they represent the first step of the clinical pipeline, aimed at evaluating the need for a biopsy, in order to avoid unnecessary surgical resections.

The aim of this work was to develop a capacitive sensor system able to measure the concentration of a specific VOC, present in a gas mixure in a closed environment and static conditions, for future application to exhaled breath samples. In this project, the target compound is Toluene, since there is scientific evidence that places this VOC between the most frequent compounds detected in exhaled breath of lung cancer patients and it could be a good candidate for the role of biomarker.
This project was carried out by combining a polymer-based capacitive sensor with a readout electronic circuit based entirely on PSoC ('Programmable System on Chip'), a platform that includes many peripherals as well as a microcontroller on a single chip. Figure 1.1 provides an overall view of the workflow of this project design.
In detail, the capacitive sensor has been realized by assembling:

- an Interdigitated Micro Electrode Array (IDA), whose golden microelectrodes are arranged in a planar circular pattern. The IDA provide the interface between the sensing layer and the electrical signal, and they offer the advantage of a widely extended area of contact with the polymeric film.

- a thin-film of Toluene-imprinted polymer aimed at the recognition of the target Toluene molecule in the air. The polymer layer is the active material, sensible to the physical property to be measured, that is the concentration of Toluene in the gas mixture.

The IDA, purchased from 'Micrux Technologies', are realized by thin-film metal technologies on a glass substrate, hence, for interfacing them with the readout electronics, a PCB (Printed Circuit Board) has been designed with 'Eagle' a software for hardware design provided by 'Autodesk'.
The sensor, together with the PCB has been mounted on a customized plastic support, realized inside our laboratory by 3D printing technique, using PLA (Polylactic Acid). The electrode support and chamber has been outlined inside 'Fusion 360', a software devoted to CAD (Computer-Aided Desig), also supplied by 'Autodesk'.
The firmware has been developed within 'PSoC Creator', the free Integrated Design Environment (IDE) by 'Cypress', and then loaded in the memory of the PSoC device for measuring changes in the capacitive sensor. The code performs a capacitance-to-frequency conversion, producing a square wave whose frequency is dependent on the external sensor capacitance, and consequently measures the frequency and sends it via serial communication to the Graphical User Interface (GUI) running on the PC, that has been written using 'Processing', in a java-based programming language, and performs computation of the capacitance value as well as real-time data visualization.
The PSoC-based capacitive measurement system has been tested to several ceramic capacitors in the pico-Farad range, and its performance was compared to the one of the commercial FDC1004Q Capacitance-to-Digital Converter supplied by 'Texas Instruments', showing an acceptable accuracy in the range from 10 to 100 pF.
After the initial calibration tests, the proposed measurement system has been used to monitor the capacitance changes of the aforementioned polymer-based sensor, while performing a series of adsorption steps, during which the sensor and its support were closed, for time intervals of increasing duration, inside a glass chamber saturated with Toluene.

The manuscript of the thesis is structured in the following way:

- **Section 2** gives an overview about the state of the art: it serves as a general introduction to current diagnostic methods for lung cancer detection, and also to the technological solutions adopted in the field of Exhaled Breath Analysis, with a focus on

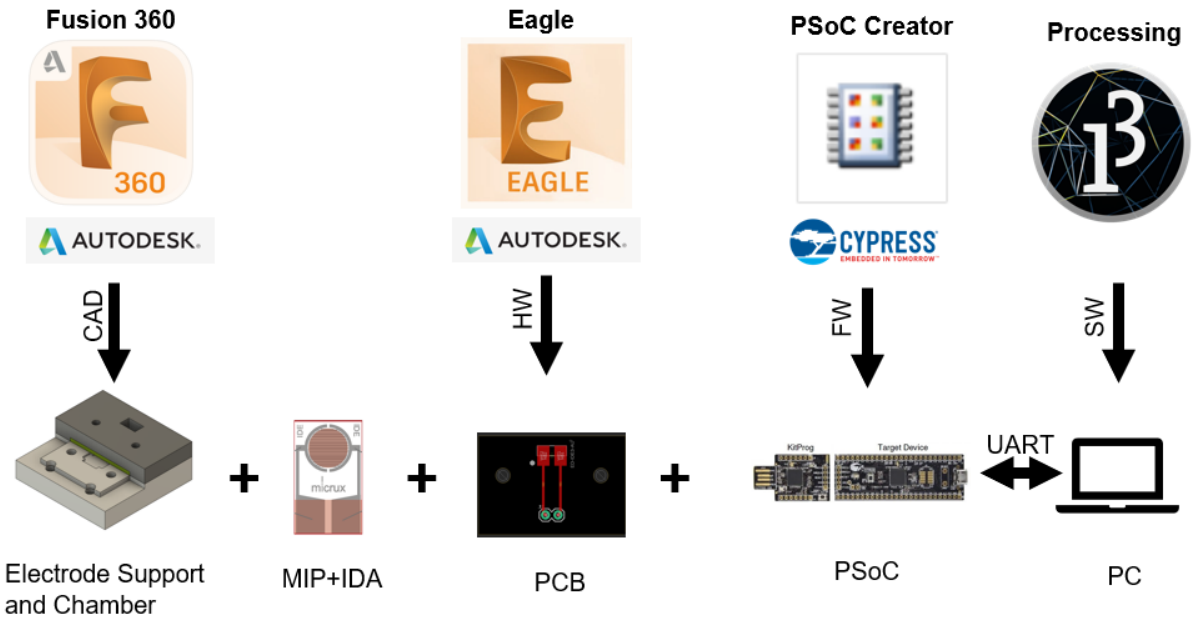

Figure 1.1: *Project Workflow*

Electronic Noses and the use of Molecularly Imprinted Polymers as recognition elements in gas chemical sensors.

- In **Section 3** is present a detailed description of the the materials and methods adopted for the development of this project, illustrating the steps of preparation of the Toluene-Imprinted Polymer used in this application, as well as the design of the customized electrode chamber, an explanation about all the components concerning the Firmware and the corresponding Software.

- **Section 4** illustrates the set up for Calibration and Measurements, performed by the developed capacitive sensor, either when coupled to the PSoC-based sensing system or with a commercially available miniaturized Capacitance-To-Digital Converter. Calibration was carried out testing the PSoC-based system on various ceramic capacitors in the pico-Farad range, and its performance was compared to the one of the commercial FDC1004Q Capacitance-to-Digital Converter supplied by 'Texas Instruments'. Measurements have been conducted for different degrees of Toluene adsorption, obtained by varying the time of exposition of the sensor inside the saturated chamber: by applying this protocol, sensors which differed in either the amount of polymer used or the technique used for template removal have been compared.

- **Section 5** contains a conclusive and overall discussion about the project, focusing on the problems that have been encountered during the design and finally giving some hints about possible future improvements and developments.

However, the work presented in this manuscript represents only the first step in the long path for developing new instrument that coulld be applied for the detection of lung cancer at early stages and widespread population screening.

Chapter 2

State of the Art

2.1 Current methods for the diagnosis of lung cancer

Currently, various combinations of multiple techniques are used for lung cancer screening purposes, particularly imaging techniques such as radiology or endoscopy [5].

- Radiological Imaging Methods:
  - **Computed Radiography (CR)**: the first part of this system is identical to standard radiography, the only difference is that, instead of using the radiographic film, the image is scanned into a digital format using a CR-specific cassette. It is much faster than standard radiography, but much slower than DR.
  - **Digital Radiography (DR)**: a new system of standard radiography requiring an integrated digital detector. It enables faster scanning and rendering with a lower radiation dose.
  - **High-resolution computed tomography (HRCT)**: enables the assessment of lung parenchyma pathology, resulting in accurate highlighting of solitary pulmonary nodules.
  - **Low Dose Computed Tomography (LDCT)**: this system is commonly used for the diagnosis of peripheral lung cancer, specially in the case of pediatric disease. It shows better specificity and sensitivity when compared to traditional chest radiography, also being less invasive, but is also have some disadvantages such as: high cost, invasiveness (because the risk associated with radiation exposure is still present), high stress for the patients and high false positive rate.
  - **Positron emission tomography - Computed tomography (PET-CT)**: Combines PET, which brings information related to the function and metabolic activity of pathological lesions, with CT, that shows their precise anatomical structures and locations.
  - **Fluorodeoxyglucose Positron Emission Tomograhy (FDG-PET)**
- Non-radiological Imaging Methods:

  - **Magnetic resonance imaging (MRI)**: it allows precise location of tumor masses while being completely noninvasve, because it does not require injection of radioactive isotopes (as used in PET, CT) that can damage tissues.
  - **Automatic fluorescence bronchoscopy (AFB)**: it is a high-precision technique that enables to detect lung cancer at early stages and also remove polyp in vivo via the associated biopsy sampling mechanism.
  - **Fibered confocal fluorescence microscopy (FCFM)**: this technique can detect scattered features of lung cancer.

- Endoscopic Methods:
  - **Endocytoscopy (EC)**: it can assist in the differentiation of various lesions.
  - **Electromagnetic navigation bronchoscopy (ENB)**: this technique is used for the diagnosis of peripheral lung lesions. It guides fine needle aspiration with relatively high sensitivity and specificity
  - **Endobronchial ultrasound-guided-Transbronchial needle aspiration (EBUS-TBNA)**: it enables highly accurate surgical evaluation.

However, the existing diagnostic procedures are either invasive, expensive or inaccurate, because in early stages of lung cancer development it is difficult to distinguish it from benign nodules based exclusively on morphological criteria [5]. There has been a lot of interest in secondary prevention, involving screening tests for the detection of early stage lung cancer. The most commonly adopted technique for screening is LCDT, but it often leads to overdiagnosis. There is a need to develop faster and non-invasive techniques for screening of high-risk population with the purpose of selecting those patients that need to enter the clinical pipeline. An ideal screening test should be sensitive, specific, minimally invasive and accessible to a large population [6].

2.2 Biomarkers for Lung Cancer

The most suitable way to perform diagnosis would be to find a biomarker that can be obtained in a noninvasive manner. According to the *'Biomarker Working Group of the US Food and Drug Administration and National Institutes of Health'*, a 'biomarker' is defined as *'a characteristic that is measured as an indicator of normal biological processes, pathogenic processes, or responses to an exposure or intervention, including therapeutic interventions. Molecular, histologic, radiographic, or physiologic characteristics are types of biomarkers.'*.

Categories of biomarkers include [4]:

- susceptibility/risk biomarkers
- diagnostic biomarkers
- monitoring biomarkers
- prognostic biomarkers
- predictive biomarkers
- pharmacodynamic/response biomarkers
- safety biomarkers

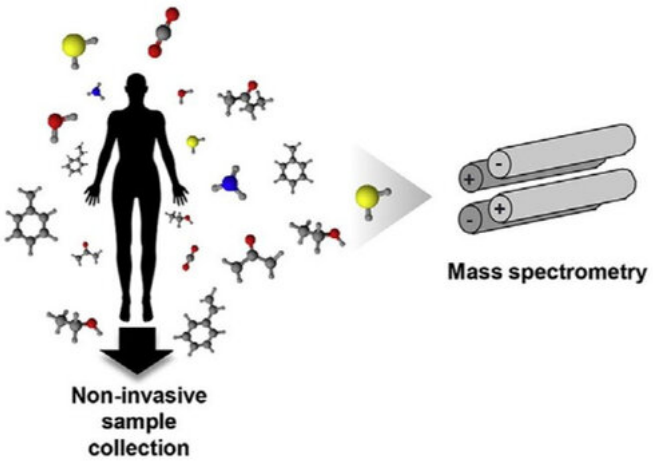

Figure 2.1: *Exhaled Breath Analysis: Non-invasive biomarkers collection [1]*

Diagnostic biomarker A diagnostic biomarker could accomplish many functions:

- it could aid in selecting high-risk patients for a CT screening programme
- it could aid in establishing a lung cancer diagnosis, especially as part of a thoracic cancer screening programme.
- when combined with info obtained from radiology and clinical data, would support multidisciplinary teams in their decisions on probability of malignancy, whenever the patients cannot be submitted to any biopsy (as in the case of severe COPD).

Predictive biomarker A predictive biomarker could be useful to predict a future treatment response. Examples of such kind of biomarkers are: Epidermal Growth Factor Receptor (EGFR), ALK and Programmed Death Ligand 1 (PD-L1).

Monitoring biomarker A monitoring biomarker could aid in the serial monitoring of treatment effect, or to distinguish between disease progression and toxicity from treatments (such as radiation or immunotherapy). It could be used in parallel to information gained from CT or PET scans. Unfortunately, in lung cancer, no such biomarkers are available, but it is currently being used in other cancer treatments.

To improve the disadvantages of existing diagnostic tools for lung cancer, there have been many attempts to detect biomarkers from the blood, sputum and bronchoalveolar lavage fluid, as well as from exhaled breath [7].

2.3 Exhaled Breath Analysis

Many recent studies have put increasing attention on the Analysis of Exhaled Breath, since it seems a very promising screening procedure for early detection of lung cancer.

Exhaled Breath is a gas containing:

- Inorganic compounds, which compose the vast majority of human breath: oxygen, nitrogen, carbon dioxide (CO_2) and nitric oxide (NO), water vapor and intert gases.

- Non-volatile molecules, present as suspended liquid-phase particles, which can be analyzed by collecting Exhaled Breath Condensate (EBC).
- Volatile Organic Compounds (VOCs), characterized by low molecular weight and relatively high vapor pressure at room temperature [8]. VOCs can be further classified into 'endogenous' (produced by internal metabolic processes within the human body) and 'exogenous' (contaminants produced from external environment, which are introduced inside the body by inhalation and absorption through the lungs or skin). There are thousands of different VOCs in human breath, but they are present at very low concentrations.

The ideal screening test would rely on the identification of biomarkers for lung cancer diagnosis in ECB or among exhaled VOCs. However, at the moment research on VOCs detection has reached a higher level of development with respect to EBC, from the technologic point of view. Since metabolic processes within the human body can be physiological but can be also induced by or altered due to disease, it is believed that endogenous VOCs, that arise from such processes, can cause a specific 'smell' or 'breathprint' for different diseases. [4], thus combinations of specific compounds could provide more informative 'biomarker panels' [5]. However, the first task is to identify which indvidual compounds should be included in the 'breathprints' that can reflect the specific pathology changes *in vivo*.

2.3.1 VOCs in other diseases

It is believed that endogenous VOCs can serve as biomarkers for different pathologies:

- **Respiratory diseases**: there have been many scientific publications reporting VOCs measured in various respiratory pathologies, including: asthma, COPD, cystic fibrosis, tubercolosis.
- **Non-respiratory diseases**: Barrett's oesophagus, inflammatory bowel disease.
  Progress has also been made in other types of cancer, located in: head, neck, oesophagus, bladder, colon, ovaries and mesothelium (the thin layer of tissue that covers the majority of internal organs) [2, 4].

2.3.2 VOCs and Lung cancer

History of Breathomics Since ancient times, the smell of human breath has been used as a way to establish the presence of a disease [5].
However, Breath Analysis (also called 'Breathomics') became of great scientific interest only in 1971, when *Pauling et al.* identified 250 different VOCs in human breath samples, by using a gas chromatograph (GC). Since then, more than 3000 different VOCs have been discovered in human breath thanks to the work of *Phillips* [9, 10].
The first attempt to link Exhaled Breath with Lung Cancer could be attributed to a trial by *McCulloch et al.* [11], which showed how trained dogs were able to distinguish lung cancer patients from healthy people with almost 100% accuracy, just by smelling their breath (hence they were aso called 'sniffer dogs'. The pioneering study on VOC in exhaled breath from lung cancer patients was published by *Gordon et al.* in 1985, using a GC-MS system.
Once identified in exhaled breath, a VOC can be considered as a biomarker if its concentration is statistically different between healthy subjects and lung cancer patients [3]. Some of the VOCs that are more likely to be candidates as biomarker for lung cancer detection are [5, 3] : *1,2,4-trimethyl benzene, 2,4-dimethyl heptane, 3-hydroxy-2-butanone, Acetone, Benzene,*

Butane, Decane, Ethanol, Heptanal, Heptane, Hexanal, Isoprene, Octane, Pentane, Propyl Benzene, Ethilbenzene, Styrene, Toluene, Undecane, Cyclohexane, Propanol, Propranolol, Isoprene.
However, at the moment both clinical and in vitro studies have failed to produce a consistent and validated list of exhaled breath biomarkers [3], since no unique compound has been found that could be useful to determine a pathologic condition, suggesting that it would be more appropriate to look for a combination of VOCs (e.i., a pattern) [12]. As a consequence, recent developments in this field exploit sensor technology and pattern recognition techniques (as in eNoses devices). These patterns need to be 'learned' by the machine using artificial intelligence (AI), analogously to the training of dogs used in the original *McCulloch*'s study. With this principle, it has now been possible to differentiate lung cancer from healthy subjects and from COPD patients [4].

Origin of VOCs Endogenous VOCs are produced by metabolic processes inside cells, successively released, transported through blood and finally excreted through lung, liver and kidney, and also emitted by skin, thus they can be measured in: exhaled breath, urine, blood, saliva and faeces [13].
Since one of the main hallmarks of cancer, together with an uncontrolled cell proliferation and resistance to cell death, is the alteration of metabolism (i.e., activation of glycolysis, meaning that the glucose uptake is considerably higher), it is reasonable to suppose that VOCs production in lung cancer patients is different from the one of healthy patients. Indeed, cancer-related changes of VOCs concentration in human breath are documented. Unfortunately, at this state, there is still a lack of knowledge about the genesis and metabolic pathways of such compounds, specially how they can be related to the biochemical pathways involved in lung cancer development. It has been found that, in order to support the high energy reqirements of tumoral cells, many metabolic enzymes and pathways are altered [6].
Michael Philips, which conducted three independent trials in order to identify VOCs in exhaled breath of lung cancer patients, noticed that, although the outcomes seemed to be inconsistent, the major biomarkers obtained were mainly alkane derivatives, which showed a decrease in lung cancer subjects. This result could be attributed to the activated cytochrome P450 (CYP450) mixed oxydase enzymes in lung cancer patients which causes an increase in catabolsim of lipid peroxidation products [3] and may accelerate the degradation of several VOCs which are markers of oxidative stress [7].
Serasanambati et al. studied the VOC profile emitted into the headspace (i.e., the gas environment trapped closely above the cell) of individual tumoral cells, comparing normal lung cells to different lines of cancer cells (characterized by different p53 genetic status). The results showed that single cells of lung cancer have unique VOC prophile, which varies temporally among genetically different cells. VOCs emission by lung cancerous cells has been investigated *in vitro* both in bulk cultures and at the level of the single cell, providing different insights that might be influenced by the heterogeneity of bulk analysis. These differences stress the need to perform VOC evaluation on all levels, from the single-cell, to a few cells, to bulk and up to real breath studies [8].
The origin of exhaled VOCs is assumed to be mainly alveolar, however, direct comparison of VOC profiles from different parts of the lung and airways is still missing.
Thus, measuring the concentration of VOCs exhaled through breath could be a way to discriminate between different diseases. This would be a screening method with many advantages: non-invasive, rapid analysis, lower cost.

Factors that may confound Exhaled Breath Analysis Unfortunately, many factors may influence Exhaled Breath Analysis results:

- **Patient-specific factors**:
  - Age
  - Airway calibre
  - Tobacco Smoking
  - Comorbidities (the presence of other diseases).
  - Lung dysfunction severity
  - Gender
- **Breath-Sampling factors**: The main limitation of exhaled breath analysis is the lack of recommended guidelines in the sampling of exhaled breath ([12]). Many techniques have been used, both for the breath sampling procedure and for the statistical analysis used to process the data, but a complete comparison between different equipment is still missing. The steps than are involved in breath analysis are:
  - exhaled breath collection (and, in many cases, storage)
  - VOCs separation and analysis
  - clinical validation of the technique

  A challenging task Detecting specific VOCs in Exhaled Breath is a task that involves many technological challenges, because of two main reasons:
  - **VOC concentration in exhaled breath is in the PPB range**: When trying to detect VOCs in exhaled breath, one of the main challenges is due to the fact that they are present in trace quantities (from PPM to less than PPB levels), thus requiring very sensitive and selective instruments that are able to detect such compounds even if in presence of those at higher concentrations [5].
  - **VOCs stability during storage is uncertain**: Concentration of VOCs can be measured either directly or after being captured and stored (e.g. via collection bags or canisters), where the latter situation requires effort to mantain VOCs stable until analysis is performed.

2.4 Technology for Exhaled Breath Analysis

2.4.1 Gas Chromatography and Mass Spectrometry (GC-MS)

In Gas Chromatography, the air sample is combined with a carrier gas, then it moves against a stationary component, where a reaction occurs, and finally the different molecules are separated [4].
Mass Spectrometry works in vacuum, by breaking the componds into their constituent ions, which are separated according to their mass-to-charge ratio by means of a magnetic field.
GC combined with MS enables both qualitative and quantitative analysis of mixed gaseous compounds, providing very accurate and precise results about the concentration of individual VOCs, but it is not suitable for application in a clinical setting, because of many reasons: first of all, this kind of analysis is highly expensive and must be performed in a laboratory, hence long time is required for the outcome to be available; then it is difficult to use, which leads to the necessity of trained personnel able to operate them and interpret the results [12].

2.4.2 Ion Mobility Spectrometry (IMS)

Ion Mobility Spectrometry (IMS) system is based on a ionising source (Ni) emitting a radiation able to break down analytes into ions, which later separate and travel towards a Faraday plate at the other end of the chamber. Each ion moves with a speed that is dependent on its specific size, mass and geometry and, when hitting the plate, generates an electrical signal. All the signals combined produce a ion spectrum, which is a fingerprint for the exhaled breath [12].

2.4.3 Electronic Noses (eNoses)

Electronic noses, also called *eNoses*, are small, portable, array-type devices. Unlike the previously mentioned techniques (IMS and GC-MS), which are aimed at identifying indvidual molecules in exhaled breath, eNoses are designed to respond to *a pattern* of chemical compounds in gaseous samples, with the aim of identifying a unique composite breath signal called 'breathprint'. Their mechanism is analogous to the human olfactory system, where the brain combines received signals generated by the interaction between specific chemicals present in inhaled air and the different receptor inside the nose in order to determine what characteristic scent pattern is sensed [14]. The operating principle of such devices relies on the adsorption of the VOCs onto an array of sensor, producing a change in each sensor's feature, which may be either conductivity, color or the frequency of oscillation of a crystal.
Electronic Noses are composed by broadly responsive arrays of such sensors, generating complex measurement data that are processed using comparative pattern recognition techniques and artificial intelligence to match measured response patterns to the ones that are already learned, in order to identify specific scents present in gas samples. Hence, a calibration phase must precede the measurement step, during which a database of breathprints is developed and later used for the training of the eNose [15].
Differences between eNoses occur at many levels [4]:

- **at the level of the air sampling technique**: almost every system needs a contained environment at the moment of sampling and measurement to prevent contamination, but, whereas some eNoses (as. for example, the Aeonose) are able to perform a real-time analysis of breath, the vast majority of instruments require a momentary storage of the gaseous sample, within a holding canister or a sample balloon.
- **at the level of methodical principles**: whereas older eNoses measured individual VOCs contrasted by other, more modern eNoses apply pattern recognition techniques combined with Artificial Intelligence. Hence, they require a training phase to be performed on a test set, followed by a validation on an independent set.
- **the different type of sensors used**: colorimetry, surface acoustic waves, conductometry.

Current level of evidence and current limitations At the moment, the question is: 'can the eNoses be useful for detection of biomarkers for population screenings purposes?'. For what concerns predictive and monitoring eNose biomarkers, research is very limited, whereas Electronic Noses have been tested both *in vitro* and in clinical trials, providing scientific evidence that they are able to detect diagnostic biomarkers pattern for discriminating cancer patients from healthy subjects, in different settings [4].
However, most of the studies have only been conducted using internal validation. Since a standardised sampling and analysis method is missing, inter-study comparison and clinical implementation is not feasible.

2.4.3.1 Colorimetry

This kind of analyzer is based on dots coated with chemically responsive dyes (e.g. metalloporphyrins on a cartridge), which can be adapted based on the targeted VOC, so that each dot is sensitive to a broad range of VOCs but with varying sensitivity. When VOCs are adsorbed onto the dots, they change their color. An image of the cartridges is taken both before and after the exposure, and the entity of the color change is converted to a digital number [12].

2.4.3.2 Surface Acoustic Waves (SAW)

The Surface Acoustic Waves (SAW) sensors emit an acoustic wave: when the surface is exposed to the gaseous sample, a reaction occurs producing a change in the acoustic wave.

Quartz Microbalance (QMC) The Quartz Microbalance (QMC) is an array of oscillating quartz crystals coated with varied metalloporphyrins, onto which the VOCs can be adsorbed, consequently changing the mass of the sensors and, as a consequence, also the oscillation frequency of the acoustic waves emitted by the crystals.

2.4.3.3 Conductometry

This technique is based either on metal oxide or polymeric sensors. In both cases, a RedOx reaction occurs, producing changes in conductivity of the sensor.

Cyranose 320 The *Cyranose 320* is is a portable analyzer containing an array of 32 carbon-black polymer composite chemiresistors. After exposure, VOCs are adsorbed onto the polymer, whose swelling produces an increase in sensor's electrical resistance. Each polymeric chemiresistor has different adsorption properties, thus a differential response is recorded across the array, producing a sample 'smellprint'.

Gold particle Nanosensor This kind of analyzer is based on a nanosensor array composed of gold nanoparticle electrodes covered with a mixture of compounds. When exposed to VOCs, a change in resistance is recorded in the sensors.

Metal Oxide Sensors (MOS) Metal oxide sensors are composed of a ceramic support tube, coated with S_nO_2. Several Metal Oxides behave as semi-conductors at high temeperature. When exposed to a gas mixture, a change in sensor conductivity can be measured, due to RedOx reactions occurring at the surface, which are determined by: the type of metal oxide and catalyst, the reacting gases and the temperature. The metal oxide sensors have many advantages such as: high sensitivity, very fast time response and recovery time, and low cost. The main disadvantages is the need for a high operation temperature (ranging from 200 °C to 459 °C), which involves a higher power consumption. Furthermore, sensitivity may be heavily affected by environmental conditions such as temperature an humidity (this is crucial since exhaled breath has a high water vapor content [2]).
The ***Aeonose***, developed by 'The eNose Company' (Zutphen, The Netherlands) is the most common eNose based on MOS, consisting of an array of 3 elements. Its main advantage is that it can be used directly by the patient breathing into the device, hence it does not require temporary storage of the breath sample, and also it offers the opportunity to transfer calibration models. This means that, once a calibration model has been developed, it can be easily transferred to other Aeonose devices, thus enabling large-scale application [15]. It

is used in combination with the software supplied by the same company, called 'Aethena', which is able to retrieve raw data from a database and performing data compression, analysis and reporting.

2.4.4 EBC Analysis

Exhaled Breath Condensate (EBC) contains 99% water vapor and a small fraction of respiratory airway lining fluid droplets.
Some genetic markers can be found in EBC. EBC Analysis is a non-invasive technique for investigating inflammation and oxidative stress biomarkers such as: hydrogen peroxide, leukotrienes, isoprostanes, hydrogen ions, prostaglandins, and nitrogen oxides.

EBC collection procedure The patient must breath tidally for 10-20 minutes though the collecting device, that could be either a tube cooled to 0°C (R Tube) or a condenser (Ecoscreen).

2.5 Molecularly Imprinted Polymers (MIPs)

Molecular Imprinting is one of the most important methods for Molecular Recognition, aimed at creating synthetic polymers that act as receptors able to achieve fast and precise detection of a target molecule. Such polymers are created exploiting surface modification techniques [16], based on the formation of specific recognition cavities in the polymeric matrix that are able to better bind the template molecules. They are called 'bio-mimetic' in the sense that they mimic the natural antibody/antigen behaviour, known as the 'lock and key' mechanism, in order to bind the target molecule [17, 18, 16]. One of the first reports about molecular imprinting was published by *Wulff and Sarhan* in 1972.

MIP synthesis There are multiple production methods, but all of them follow the same basic outline:

- ASSEMBLY: the template (e.g., the target molecule) is bound, covalently or noncovalently, to a functional monomer of the host polymer, producing the 'pre-complex'.
- POLYMERIZATION: In presence of the cross-linker, pre-complex undergoes polymerization, thus obtaining the polymeric matrix. The template directs the positioning and orientation of the structural components via a cross-linking agent.
- TEMPLATE REMOVAL: the template molecule is removed from the polymeric matrix by means of a suitable desorption agent. It leaves some target-specific cavities in the host polymer that will be available as recognition sites for future rebinding of target molecule with higher selectivity, since those cavities are complementary to the template molecules in shape, size and steric configuration (Steric effects are nonbonding interactions that influence the conformation and reactivity of ions and molecules. They result from repulsive forces between overlapping electron clouds).
- REBINDING: the MIP is exposed to a complex sample containing a certain amount of the target molecule, which will be selectively uptaken by the cavities.

Some of the advantages of MIPs are the cost-effectiveness, the fact that they can be cleaned and re-used, and the great flexibility they offer in the design, since they can be synthesized by different combinations of: functional monomers, cross-linkers, initiators and solvents.

The choice of a particular combination of the aforementioned elements will obviously affect the quality and the features of the resulting MIP. For example, interactions between the host and target creating the imprint may have either covalent or non-covalent nature: the difference between the two methods is mainly in the chemistry needed to remove the template from the MIP, but it is also true that the covalent synthesis is expected to produce a more homogeneous set of rebinding cavities and, potentially, more target-specific MIPs. In a MIP, specific sites can be created for various targets such as: amino acids, proteins, enzymes, hormones, antibodies, nucleic acids, bacteria, viruses, drugs, metal ions, toxins, antibiotics, pesticides, and so on.

According to *Baggiani et al*: the existence of the template in the pre-complex mixture helps to improve the interactions that already existed in the corresponding Non-Imprinted Polymer (NIP) [19]. This means that:

- If the NIP does not bind the target molecule, then the corresponding MIP will display a *weak* imprinting effect;
- If the NIP binds the target, then the MIP will display a *strong* imprinting effect.

Important parameters: Imprinting Factor, Binding Capacity, Response Time.

- Imprinting factor (IF): the ratio of binding of the template in the MIP to its binding in the NIP.
- Binding capacity (BC): the ratio of the concentration of target molecule adsorbed from the test solution divided by the initial concentration of that solution (multiplied by 100).
- Response time (RT): usually it is defined as the time required to reach 63.2% of the final signal, starting from the time the stimulus is applied.

Problems Some problems that should be taken into account:

- Occurrence of nonspecific binding to the templated material: since the host polymer itself is an adsorbent, and some, even weak, interaction with the target molecule is unavoidable.
- Non-homogeneous binding sites.
- The need to extract the target molecule from the MIP, since the presence of any unextracted target may interfere with the ability to sense the rebinding

Definition of Sensor A 'sensor' is defined as: *'a device which detects or measures a physical property and records, indicates, or otherwise responds to it'* [16]. In particular, for a **chemical sensor** the 'physical property' is the presence of the target molecule, which means that the chemical sensor is able to convert chemical signal depending on analyte concentration into a measurable analytical signal. Any sensors contains two important components:

- **Recognition Element** (or **Receptor**), which interacts with an analyte and is responsible for the capture of the target molecule. The choice of the receptor depends on the target molecule. Chemical sensors are sorted according to the Recognition Molecules used.
  - Natural recognition elements: Enzyme, Antibody, Nucleic Acid, Cell, Aptamer

  - Synthetic recognition elements: MIPs (inspired by the natural mechanisms of antigen/antibody interactions)

- **Transducer** : able to convert the binding event into a measurable signal.

The sensors can be classified as: electrochemical, piezoelectric (e.g., QCM sensors), optical, magnetic, micromechanical and thermal.
Sensor technology offers many advantages, such as: exceptional sensing performance, user-friendly operation, fast response, high sensitivity and specificity, portability, and real-time analysis. In particular, for the electrochemical sensors, some of the advantages include [18]: size, portability, low cost. Thanks to sensor technology development, the biomolecule testing can be moved from large centralized laboratories to point-of-care devices, that can be used by patients themselves when they are at home, or in a doctor's clinic. In future research these sensors can be developed in the form of hand held devices where the patient can test and see the results by her/himself without medical assistance.

MIP-based Sensors Molecularly-Imprinted-Polymer-based Sensors (MIP-based Sensors) are chemical devices based on the incorporation of MIPs, as the active elements whose final goal is analyte recognition, coupled with a transducer platform, aimed at monitoring changes in the recognition element, which can be of different nature: electrical, electrochemical, optical, or gravimetric.
MIP sensors can be used for monitoring the environment, but they also offer the opportunity of selective and sensitive detection and monitoring of VOCs in a non-invasive manner, being a promising approach for the detection of several molecules.
This method has great versatility, since it is possible to imprint a variety of biomolecules with different size, 3D structure, physical and chemical features and it can lead to the development of novel, rapid, reliable, cheap, selective and sensitive diagnostic tools. There is scientific evidence about elecrochemical MIP-based sensors able to target: viruses, glucose, myoglobin, dopamine, creatinine, naloxone, sarcosine, cocaine.
MIP-based sensing is attractive because of its many advantages: specificity, selectivity, cost efficiency, physical and chemical stability (with respect to the biomolecules), ease of preparation and applicability of the method for diverse biomolecules. According to the literature, they should be able to provide low detection limit values (close to the conventional methods).

2.6 Interdigitated Electrode Arrays (IDA)

Chemical interdigitated electrode sensors Chemical interdigitated electrode sensors can be either capacitive or resistive [20]:

- **Resistive**: the sensing layer must be partially conductive, as it acts as a resistor between the microelectrodes of the interdigitated pattern. Resistive Chemical Sensors require a flow of current through the sensing layer when exposed to analyte, hence the conductivity of the film changes and the measured electrical resistance R also changes, responding to different concentrations of the analyte. A resistive interdigitated electrode may be modeled as a chain of individual resistors arranged in parallel [20].

- **Capacitive**: the sensing layer must be essentially NON-conductive, because it acts as a dielectric between two parallel interdigitated electrodes. The output measures a change in capacitance of the sensor.

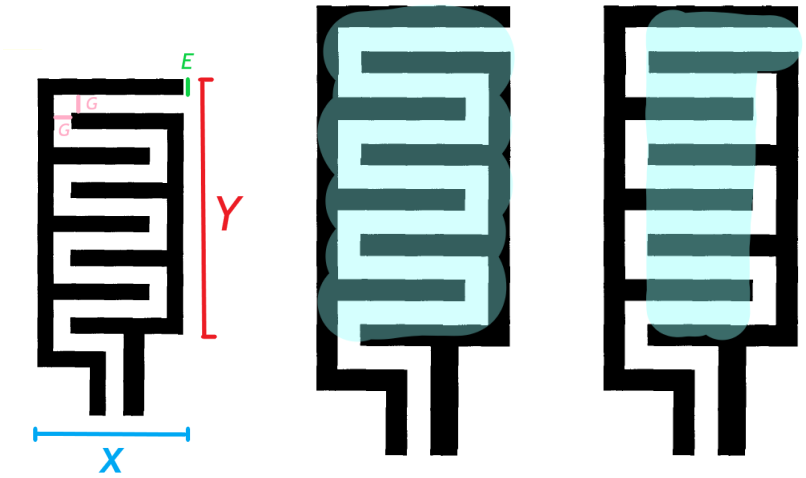

(a) Relevant dimensions for the rectangular pattern.

(b) Expected Sensing Area

(c) Actual Sensing Area (losses at the corners)

Figure 2.2: *Interdigitated Electrode Array - Generic rectangular pattern.*

Capacitive Chemical Sensors Capacitive Chemical Sensors are composed by an insulating chemically sensitive thin film that is deposited over the IDA: this layer acts as the dielectric in the resulting interdigitated electrode capacitor, since the dielectric constant of the sensing layer changes when exposed to different analytes in different concentrations, producing a cariation in the capacitance C, which is measured as a function of analyte concentration. The response curve is given by the variation of capacitance of the sensor, plotted versus time, while varying temporally the concentration of the analyte (or the partial pressure of the analyte in the air).
Such kind of sensors are very common for measuring relative humidity, but they can also be adapted for targeting a different analyte, such as a VOC: depending on the chemical behaviour of the thin film dielectric deposited over electrodes and the gap between them (see figure 2.2a), capacitive sensor that can detect any analyte in the gas or liquid phase.
There are many advantageous features, such as the fast time response, the reversibility, and the linear dependency of C from the partial pressure of the analyte (or concentration). A capacitive interdigitated electrode may be modeled as a chain of individual C arranged in parallel [20].

Efficiency of IDA design At the moment, there is no standard expression for the efficiency of IDA design. Figure 2.2a shows the design of a generic interdigitated electrode sensor, highlighting the important dimensions: Y is the overall electrode height, X the overall electrode width, G indicates the gap thickness, and E the microelectrode thickness (e.g., the width in correspondence of the serpentine 'fingers').
Sensing material is commonly deposited over the entire surface, but only the material lying in the 'sensing area' actually reacts to the analyte. Hence, the actual sensing in a capacitive or resisitive sensor occurs only at the serpentine gap area, there is no effect from the sensing layer deposited directly on top of the interdigitated electrodes, meaning that only a small fraction of the total sensor area actually senses the analyte. The true sensing area is actually less than expected, because G is not constant: between the two electrodes corners, gap width is higher than G, and its max deviation is: $\sqrt{2}G$ (= 1.4142G. Hence, the sensing material

between corners is inactive in response to analyte, as a consequence of this increased gap width.
A possible solution to the issue of loss of sensing area close to the corner is smoothing and rounding the corner of the rectangular pattern [20], and moreover designing novel interdig-Itated electrode array whose 'finger are arranged in a circular pattern, such as the ones provided by Micrux [21] that have been chosen for this application.

Chapter 3

Materials and Methods

The following chapter illustrates the modules of the developed measurement system architecture.

3.1 Reminder on capacitive sensing

A capacitor is an electrical component, consisting of a pair of conductors (armatures or plates) separated by an insulating layer, that is able to store energy in the electrostatic field existing between its plates. If a voltage V is applied to the armatures, a field is generated within the dielectric: the charge Q that is present on each armature, in equal amounts but opposite sign, is proportional to the applied voltage, and the constant of proportionality, characteristic of a particular capacitor, is called 'electrical capacitance' C.

$$C = \frac{Q}{V} \qquad [F] \tag{3.1}$$

The electrostatic energy accumulated by the capacitor is localized in the dielectric material which is interposed between the plates. The electric field lines direction goes from the higher voltage potential plate towards the lower voltage potential one. For a capacitor with flat and parallel faces, neglecting the losses at the edges / perimeter, the capacitance:

$$C = \epsilon_0 \cdot \epsilon_r \cdot \frac{A}{d} \qquad [F] \tag{3.2}$$

Being $\epsilon_0 = 8.854 \cdot 10^{-12}$ [F/m] the dielectric constant in vacuum, ϵ_r the dielectric constant of the insulating medium between the two plates, A the exposed surface of each plate and d the distance between them. The parallel plate equation does not take into account the fringing effect, as it would be too complex, but is a good approximation if the distance d between the plates is small compared to the other dimensions of the plates so the field in the capacitor over most of its area is uniform [22].
Capacitive sensing has benefits, including very low power consumption and sensing range, but there are also some critical aspects that must be taken into account [23], such as: parasitic capacitance, external interference, and the influence of temperature and humidity. All these issues should be addressed when designing a capacitive measurement system. However, there are ways to overcome these problems (for example, by means of an active shielding). When trying to minimize any external interference seen along the line, the length of the signal path between the capacitive sensor and the point at which measurement is performed should be as short as possible (however, for application requiring the signal paths to be necessarily long,

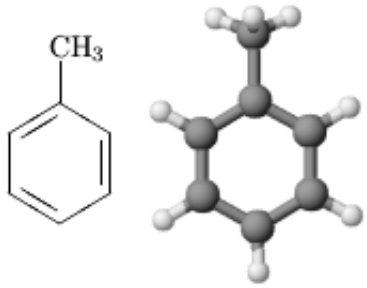

Figure 3.1: *Toluene: Chemical Structure and Model of the Molecule*

Chemical formula	C_7H_8
Molecular weight	92.15 g mol^{-1}
Vapor Pressure	2.8 kPa (at 20 °C)
Melting point	-95 °C (178 K)
Boiling point	111 °C (384 K)
Appearance	colorless liquid
Odor	sweet, pungent, benzene-like
Odor threshold	2.9 PPM

Table 3.1: *Toluene features*

the Capacitance-to-Digital Converter FDC1004 allows parasitic capacitance compensation up to 100 pF [24]).

3.2 Toluene-Imprinted Polymer

The recognition element of the sensor system is the Toluene-imprinted polymer, which has been realized at the 'CFA Lab' (Applied Physical Chemistry Lab) of the 'Department of Chemistry, Materials and Chemical Engineering' (DCMC) 'Giulio Natta' of Politecnico di Milano, by the team of prof. Francesco Cellesi, Isabel Espinoza and Marco Maroni (`https://cfalab.chem.polimi.it/`).

3.2.1 Toluene

Toluene (C_7H_8), also known as 'toluol' or 'methylbenzene' (according to the IUPAC systematic nomenclature) is an aromatic hydrocarbon. It is a mono-substituted benzene derivative, consisting of a methyl group (CH_3) attached to a phenyl group.

Toxicology Toluene is a colorless, water-insoluble volatile solvent, which is widely present in paints, paint thinners, fingernail polish, lacquers, adhesives, and rubbers [25]. It is a toxic indoor air pollutants and, even at very low concentrations, it can be harmful to health: inhalation of toluene in low or moderate levels can cause tiredness, confusion, weakness, drunken-type actions, memory loss, nausea, loss of appetite, hearing loss, and colour vision loss. However, some of these symptoms usually disappear when exposure is stopped. Instead, acute exposure to toluene can lead to central nervous system disorders, liver, and kidney

damage [25]. For this reason, the 'World Health Organization' (WHO) established a limit of 70 PPB for the concentration of the toluene that can be present in the indoor air [26] and the 'Occupational Safety and Health Administration' (OSHA) set the 8-hour time-weighted average exposure limit at 100 PPM [25].

Metabolism in humans Around 25% - 40% of Toluene that is introduced inside the body from exogenous sources is usually exhaled via the lungs without undergoing any modification, but the majority is metabolised and excreted via other pathways. Five members of the the cytochrome P450 (CYP) superfamily (CYP1A2, CYP2B6, CYP2E1, CYP2C8, and CYP1A1 enzymes) are important in toluene metabolism, being involved in hydroxylation of Toluene to benzyl alcohol.

Toluene and Lung Cancer Toluene has been reported as one of the most suitable candidate biomarkers for lung cancer detection [3]. The level of Toluene measured in exhaled breath of healthy non-smoker subjects is around 20-30 PPB, whereas in lung cancer patients it can reach 80-100 PPB, which is a value considerably higher [27, 28, 29, 30]. Hence, detection of Toluene is of great importance both for cancer diagnosis and air quality monitoring [25].

3.2.2 MIP-Sensors: Preparation Procedure

The measurement protocol was aimed at investigating the system's response throughout all the steps concerning the preparation of the sensor, starting from the bare and clean electrode and up to the final assembly with the Toluene-imprinted polymer, in order to fully characterize the proposed MIP-based capacitive sensor.
The steps for the preparation of Toluene-Imprinted Polymer film and its deposition onto the IDA are the following:

1. **Cleaning**: First of all, in order to remove any possible contaminant, all the electrodes, both New (N) and Used (U), have been treated through five cycles of sonification, each cycle consisting of 5 min of immersion in de-ionized water followed by 5 min in ethanol (C_2H_6OH). At the end of this phase, clean electrodes are obtained (labeled N1 and U1).

2. **Functionalization**: After cleaning procedure, electrodes are immersed in a solution containing the functional monomer, *Bis(2-methacrylol)OxyethylDiSulphide* (BODS). Thanks to its ability to bond the gold electrode surface, this monomer is needed to ease the following step of the anchorage of the thin-film MIP over the serpentine od the IDAs. Thereby, functionalized electrodes are obtained (labeled N2 and U2).

3. **Deposition of the thin-film imprinted polymer**: A certain amount of polymeric solution (i.e., the host-polymer combined with the template/toluene) is dropped onto the functionalized electrodes, and immediately followed by polymerization;

4. **Template Removal**: In order to create the recognition cavities inside the polymer that enable future rebinding, Toluene must be removed from the imprinted layer, either by means of a solvent or by evaporation inside a vacuum heather.

Several sensors have been assembled with different features, by varying some parameters in the aforementioned preparation procedure:

- in the **state of the IDA**: to investigate the difference between the use of a freshly new electrode with respect to an electrode which was already used (e.g., already submitted to the deposition of the thin-film MIP) and had been cleaned for further reuse.

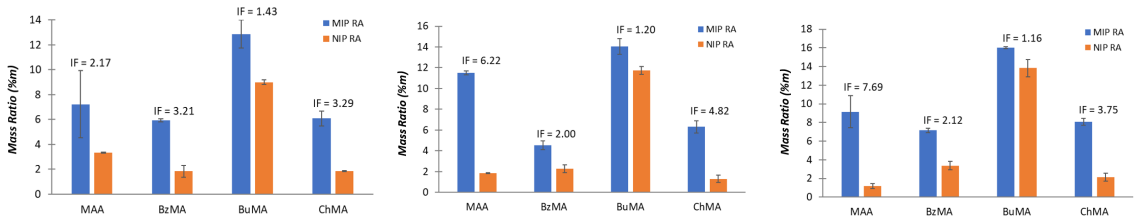

(a) TGA: **(b)** UV-Spectroscopy **(c)** HPLC

Figure 3.2: *MIP characterization for different functional monomers used in the formulation.*

- in the **amount of MIP used to build the active layer**: in order to study the influence of the thickness of the polymeric film, three different volumes (V1 = 4µL, V2 = 8µL, V3 = 12µL) of polymeric solution (i.e., the host-polymer combined with the template/toluene) have been deposited onto the functionalized electrodes. In order to produce the thinner layer, corresponding volume V1, a 4µL drop of polymeric solution was deposited on the cleaned chip, immediately followed by polymerization; then, the other volumes V2 and V3 were created by repeating the same drop deposition and polymerization steps for, rispectively, two and three times.
- in the **method adopted for template-removal**: in order to investigate how the sensor response is affected by the technique used, in the final step of MIP preparation, to extract Toluene from the imprinted layer, two different methods have been used:
  - By putting the assembled chips inside the vacuum heater (at T = 30 °C), so that toluene evaporates (thus obtaining the sensors labeled N-vac, U-vac);
  - By using acetone, an organic solvent (thus obtaining the sensors labeled N-sol, U-sol).

The system has then been used to monitor the capacitance variations in the MIP-based sensors, that had been assembled with different characteristics, while performing a series of adsorption steps, during which each sensor was mounted on its support and then closed, for time intervals of increasing duration, inside a glass chamber saturated with Toluene. E exposition time intervals of 15, 30, 60 and 120 minutes were labeled, respectively, RA1, RA2, RA3, and RA4.
Each sensor's capacitance was monitored by fastly picking measurements in the small amount of time between two consecutive adsorption phases of the whole procedure. once the sensors are extracted from the saturated chamber, measurements must be performed as fast as possible, since Toluene has high volatility and it could disperse in a very short time.

3.2.3 MIP characterization

The Toluene-imprinted polymer that we have chosen for the assembly of the proposed MIP-based capacitive sensor has been synthesized by the Team of Prof. F. Cellesi, I. Espinoza and M. Maroni in the 'Laboratory N.401' of Chemical Department of the Polytechnic University of Milan, who investigated the chemical behaviour of the bulk polymer (bulk polymeric sample, with mass in a range of 10-20 mg) by means of three different analytical tachniques: 'dinamic Thermal Gravimetric Analysis' (dinamic TGA), 'UV Spectroscopy' and 'High Performance Liquid chromatography' (HPCL).

- Dynamic TGA is a technique that submits the sample to a linear temperature prophile over time, while monitoring the variation of its mass.

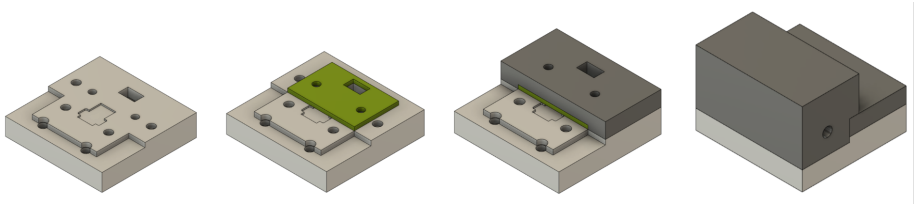

Figure 3.3: *Electrodes Support and Chamber*

- Ultraviolet-Visible (UV-Vis) Spectroscopy: it exploits light in the visible and adjacent ranges, and analyzes the sample based on the absorption or reflectance in the visible range, which directly affects the perceived color of the chemicals involved.
- High-performance liquid chromatography (HPLC): analytical technique that relies on pumps to pass a pressurized liquid solvent containing the sample mixture through a column filled with a solid adsorbent material. Each component in the sample will show different flow rate, and can consequently be separated.

This part of the analysis was kindly provided to us by their team, in order to confirm that the employed MIP's formulation with good chemical response in response to toluene adsorption. They studied different MIP formulations based on the following functional monomers:

- MMA (Methacrylic Acid);
- BzMA (Benzyl methacrylate);
- BuMA (Butyl methacrylate);
- ChMA (Cyclohexyl Methacrylate).

The figure 3.2 shows the quantification of Toluene, expressed as percentage mass ratio between template and polymer masses, through the three different analytical techniques mentioned above: thermal (TGA), spectroscopic (UV-Vis) and chromatographic (HPLC) analysis.
The histograms have been repeated for different MIP formulations (MAA, BzMA, BuMA and ChMA) each against the corresponding Non-Imprinted Polymers (NIPs) after re-adsorbtion of Toluene (RA). It also indicates the value of the Imprinting Factor (IF), which represents the ratio of percentage mass mean of MIP to NIP.
Note that TGA showed that greater and faster loss in weight which registered for MIPS with respect to NIPs, thus confirming the capability of MIPs to improve the selectivity in the re-adsorption of the template.
From the TGA outcomes, the Cyclohexyl Methacrylate (ChMA) seems to be the monomer resulting in a MIP with the higher selectivity. However, from the other two analysis that have been conducted, MAA (Methacrylic Acid) appears to be the best solution, and this brought to the final decision to use the MAA-based formulation for the realization of the Toluene-Imprinted Polymer in this application.

3.3 Electrode Support and Chamber

A customized plastic support was realized for keeping the electrodes in position and constantly an electrical contact with the PCB when performing measurements, together with a gas chamber, which was thought to be useful for future experiments in which the presented

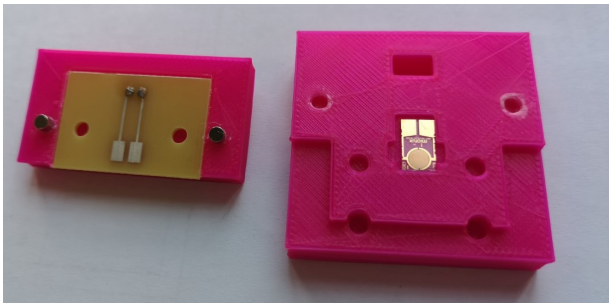

(a) Left: the Top cover, with the PCB already inserted. Right: The Base, containing the Micrux IDA.

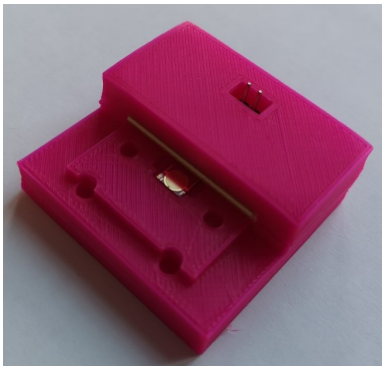

(b) Electrode Support: Top mounted onto the Base by means of Neodymium Magnets

Figure 3.4: *Elextrode Support, realized by 3D printing in PLA (Polylactic acid).*

system would be applied to real exhaled breath samples in a closed hydraulic circuit. The case provides a simple 2-wires connection for interfacing the IDA's PCB with the following readout electronics implemented inside the PSoC.
The chamber and support were designed using 'Fusion 360', a cloud-based CAD/CAM tool, provided by 'Autodesk' industrial company. This software combines organic shapes modelling, mechanical design and manufacturing in one comprehensive package, thus it is an excellent tool for the precise modeling of 2D and 3D objects, as well as for collaborative product development.
Every plastic piece has been realized using the 3D printing technique, which makes it possible to realize complex shapes while limiting costs, indeed the customized chamber and support has been realized with the 3D Printer available in our Laboratory ('Robox' 3D Printer, produced by 'CEL'), bu using PLA (Polylactic acid, or polylactide), a thermoplastic polyester material supplied by 'Robox', since it is the most widely used plastic filament material in 3D printing (probably it has become a popular material due to it being economically produced from renewable resources).
The electrode support (base Area = 45x44mm, height = 10mm) has been designed in a way that it enables two different closing systems with the top cover: with the first one, the PCB needs to be fixed manually between the base and the top pieces, with the aid of two screws, whereas the other design only relies on the attractive force of neomydium magnets that are mounted both on the top and on the base, hence providing a very fast clamping solution, that resulted to be critical while performing the series of adsorption step measurements on the sensors.

3.4 Hardware

3.4.1 Interdigitated Microelectrodes

In this sensor system, the Toluene-imprinted polymer must be coupled with the InterDigitated Electrode Array (IDA, fig.3.5a) fabricated by thin film technologies on a glass substrate by 'MicruX Technologies' (product code is 'ED-IDE3-Au') [21], consisting of two individually addressable thin-layer gold strips, the Working Electrodes 'WE1' and 'WE2': each working electrode is provided with a pad for electrical connection (PAD dimension= 2x2.5mm), and a series of micro-electrodes (microelectrode width = 5μm, with gap = 5μm), designed in

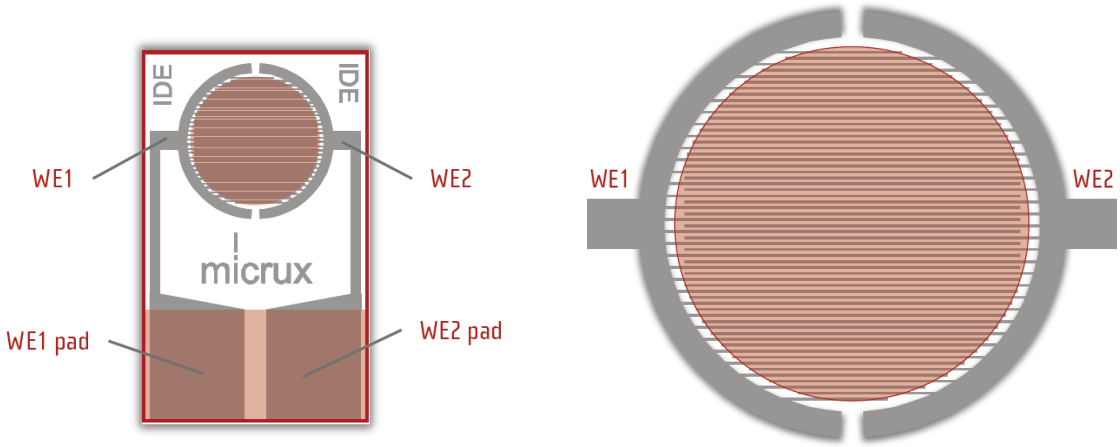

(a) Electrodes **(b)** Zoom on the Interdigitated Array

Figure 3.5: *Circular Interdigitated MicroElectrode Array (ED-IDE3-Au) by Micrux Technologies*

Standard dimensions	10 x 6 x 0.75 mm
Substrate Material	Glass
Protective layer	SU-8 resin
Electrochemical cell diameter	3.5 mm
Electrode material	Gold
Microelectrode width	5 µm
Microelectrode gap	5 µm
Number of feet	180 pairs
Thickness	50/150 nm

Table 3.2: *Micrux Electrode features*

a planar circular interdigitated pattern (fig.3.5b). The surface of the electrodes is covered with an nsulating protective layer made of SU-8 resin, except from the pads and the circular sensing area.
Some of the electrodes features are listen in Table 3.2. The overall chip dimensions are: 10mm height, 6 mm width and 0.75mm thickness, considering also the glass substrate. Depending on the characteristics of the coupled polymer, the interdigitated electrodes can be useful either for impedance, capacitance and conductivity measurement: in this case, being the Toluene-imprinted polymer completely dielectric (since it has not be doped with any conductive material), the resulting sensor is expected to exhibit a variable capacitance when exposed to gas mixtures containing Toluene. The sensing area will be given by the coupling of the MIP layer onto and in between the combs of the interdigitated portion of the electrodes.

3.4.2 PCB for interfacing the IDA

In order to provide a cabled electrical connection of the planar IDA with the readout electronics, an expremely basic 'Printed Circuit Board' (PCB) has been designed using 'Eagle', an electronic design automation (EDA) software provided by Autodesk, that enables to draw the schematic diagrams corresponding to the hardware circuit board, by component placement, PCB routing, and comprehensive library content. It consists of a minute 20mmx30mm board, providing a very simple electrical interface by means of two copper pads with footprint

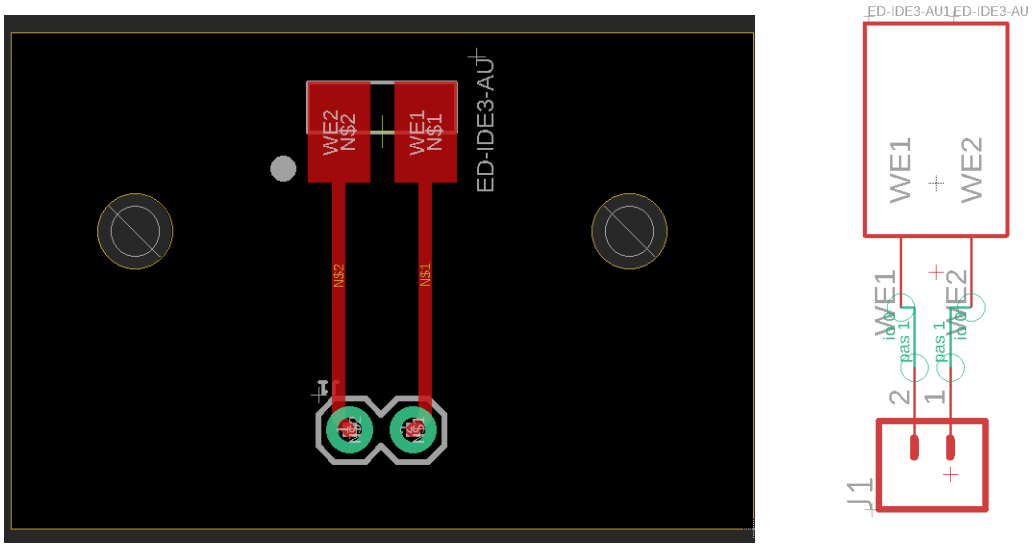

(a) PCB: Board **(b)** PCB: Schematic

Figure 3.6: *Hardware: PCB for interfacing the IDA electrodes.*

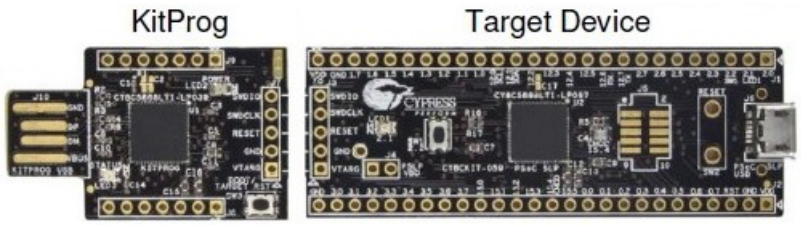

Figure 3.7: *Programmable System on Chip (PSoC) 5LP: CY8C58LP, by Cypress Semiconductor*

2mmx4mm, that is longer with respect to the two planar gold pads of the Micrux electrode (2mmx2.5mm), two routes of 20mils width (i.e.: 0,508mm) and a 2-pin male connector to attach the cables. Two lateral holes have been introduced to allow mounting the PCB between the Top and the Base of the customized plastic support by means of screws.

3.4.3 PSoC

The core of the sensing system is the PSoC 5LP (CY8CKIT-059 PSoC5LP Prototyping Kit): 'PSoC' stands for 'Programmable System on Chip' , which is a prototyping platform system for embedded control design produced by 'Cypress Semiconductor Corporation' Company, integrating configurable analog and digital peripherals, memories and a PSoC5LP Microcontroller on a single chip. It belongs to CY8C58LP ultra-low-power family of devices, in fact it needs only from 1.71 to 5.5 V voltage supply [31]. It is composed by 2 main parts: the KitProg and the Target Device. The KitProg board is used to program and debug the target PSoC 5LP device. It connects:

- to the USB port of the PC, through the PCB USB connector,
- and to the Target device through the SWD interface, which enables, after programming is completed, to separate the KitProg from the Target, thus maintaining only the latter for embedded applications.

Number of Channels	4
Input Range	±15 pF
Measurement Resolution	0.5 fF
Maximum Offset Capacitance	100 pF
Programmable Output Rates	100/200/400 Samples/s
Maximum Shield Load	400 pF
Supply Voltage (range)	[-0.3;6]V
Supply Voltage (recommended)	3.3 V
Temperature Range	[-40 ; 125] °C
Current Consumption (Active mode)	750 µA
Current Consumption (Standby)	29 µA
Interface	I^2C

Table 3.3: *Some features of the Capacitance-to-Digital Converter*

It is equipped with [31]: a 32-bit ARM Cortex-M3 core, a DMA controller and digital filter processor (at up to 80 MHz), programmable digital and analog peripherals, and a very versatile I/O system, providing flexible routing of analog or digital peripheral functions to any pin.

3.4.4 Capacitance-to-Digital Converter I.C.

The FDC1004Q is a 4-channel capacitance-to-digital converter (figure 3.8a), supplied by 'Texas Instruments', which, although being a very low power and cheap I.C. and able to Instruments is able to perform capacitive measurements of grounded capacitors with very high resolution (up to 0.5 fF). Each channel has a full scale range of ±15 pF and can handle a sensor offset capacitance of up to 100 pF, which can be either programmed internally or can be an external capacitor for tracking environmental changes over time and temperature [24]. The device has a very small footprint , thus it can be used also in space-constrained applications, and available in a 10-pin VSSOP package, that is, with 0.5mm spacing. For convenience, it has been soldered on a SOP to DIP adapter (provided by 'Winslow Adaptics', see figure 3.8b) with inter-pad distance 2.54mm, thus enabling their use on a standard prototyping breadboard.
It features an I^2C interface for interfacing to the PSoC 5LP microcontroller. Some other features of the device are listed in Table 3.3. The CapConverter has been configured using the PSoC-based code developed by Davide Marzorati and available at the GitHub online repository: `https://github.com/dado93/PSoC-FDC1004Q`, together with the Library domuntation `https://dado93.github.io/PSoC-FDC1004Q/index.html`.

3.5 Algorithm: Method of the Time constant for Capacitance Measurement

This project implements a measurement of an external capacitor using a Delta Sigma ADC, based on calculation of the time constant of a series RC circuit.

Operating principle The unknown capacitor, that should be fully discharged prior measurement, is charged through a series resistor R. When it reaches 63.2% of its maximum, the

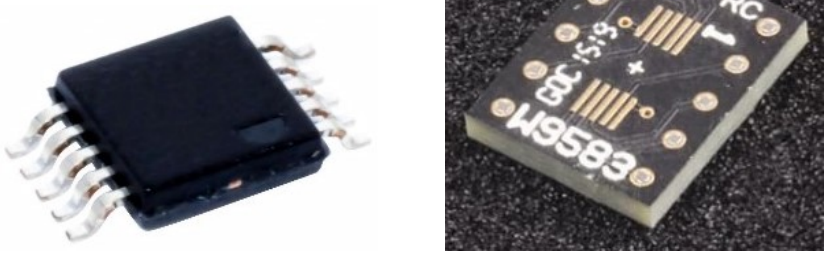

(a) The FDC1004Q Capacitance-to-Digital Converter

(b) Breakout Board: SOP to DIP Adapter by Winslow Adaptics.

Figure 3.8: *Capacitance to Digital Converter.*

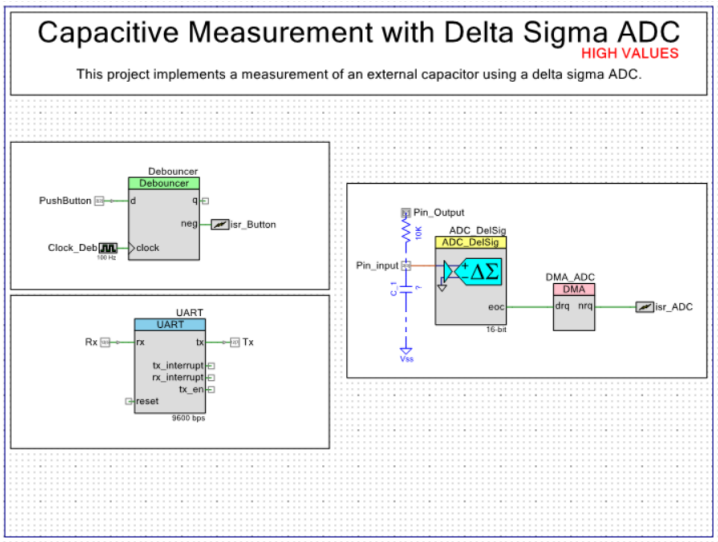

Figure 3.9: *Capacitance Measurement based on the Time Constant, implemented with Delta Sigma ADC (Top Design).*

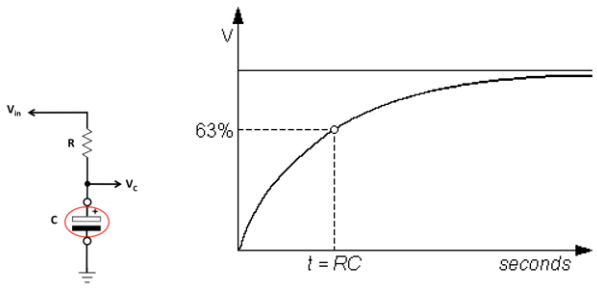

Figure 3.10: *Capacitance Measurement based on the Time Constant*

Input Mode	Single ended
Conversion Mode	continuous
Resolution	16
Conversion rate	6000 SPS
Internal Clock frequency	684.000 kHz
Input Range	Vssa to Vdda
Buffer Mode	Rail to Rail
Buffer gain	1

Table 3.4: *Configuration of the Delta Sigma ADC Component:*

time elapsed corresponds to the value of the time constant of the circuit: tau = RC. Hence, knowing the value of the series resistance R, C can be computer as: C = tau/R.

The TopDesign of the circuit is shown in figure 3.9: it needs only an external Resistor component: R = 10 kω, connected between the two digital pins Pin_Output and Pin_Input, since the remaining part of the circuit is based on PSoC internal resources, including the 16-bit Delta Sigma Analog to Digital Converter (ADC), DMA, Debouncer an the UART modules.

Debouncer Digital Input Pin 'PushButton' is connected to the on-board user button already present on the PSoC platform. Being a mechanical switch, the user button may tend to make and break connections for a finite time before settling down to a stable state. In order to protect the following digital circuit by the multiple state transitions caused by contact bouncing, a Debouncer component is introduced between the the 'PushButton' pin and the following ISR block. The Debouncer module (internal clock 100Hz) is set to detect negative edges from the user button, but it waits for a predetermined period of time before passing the signal, thus generating a clean output, so that the following ISR will respond to only one pulse generation performed by the pressing of the switch.

DMA (Direct Memory Access) The DMA (Direct Memory Access) component is used to allow data transfers from the 16-bit ADC Peripheral to RAM memory, with no CPU intervention. The PSoC provides up to 24 distinct DMA channels, that are able to transfer data independently one from eah other. Each channel has a chain of Transaction Descriptors (TD). DMA component is useful to unburden the CPU of the task of transferring data when data needs to be transferred in a predictable way that can be set up beforehand. In this project, three transaction descriptors (TDs) are chained together. transaction descriptors are...

This program starts charging the capacitor through R by setting Pin_Output high when the user button is pressed, then ADC converts the analog signal at Pin _Input with a 6kHz sampling frequency, DMA transfers all the collected samples to an array inside the RAM Memory (array dimensions: Num x N_SAMPLES).

At startup, the program starts all components (UART, ADC) and configure DMA for data transfer from ADC to RAM, enable global interrupts and start the interrupts.

- Button_ISR: sets a flag, which is polled in the main program to check whether the on-board button has been pressed or not by the user.

N_SAMPLES	2040	Number of samples for each DMA transaction descriptor (TD)
DMA_TRANSFER _COUNT	2·N_SAMPLES	Total number of bytes to transfer for each TD
NUM	3	Number of transaction descriptors chained together (TDs)
N_SAMPLES_TOT	NUM·N_SAMPLES	Total number of samples that are recorded is 6120
DMA_BYTES_PER_BURST	2	Two bytes are transferred at a time (the 16-bit sample from ADC)
DMA_REQUEST_PER_BURST	1	Transfer only on new request (by the EOC output of ADC)
Source	DeltaSigma ADC (a peripheral)	The source is a Peripheral (the ADC DeltaSigma)
Destination	SRAM Memory	The destination is an array in RAM Memory

Table 3.5: *Configuration of the DMA Component:*

- DMA_ADC_ISR: sets the flag indicating the completion of a transaction by the DMA.

When the user presses the button, DMA is enabled and Pin_Output is set high, thus charging the external capacitor though the 10kOhm resistor. The voltage across the capacitor, that is expected to raise exponentially, is measured at Pin_Input and converted to a digital value by the DeltaSigma ADC. The EOC output ('End of Conversion') of the ADC shows a rising edge everytime a 16-bit sample and consequently, being connected to the DMA input,triggers a hardware request for DMA to start transaction of the sample to RAM memory. When the DMA has completed the transfer of the 6120 samples, an ISR sets a flag to indicate it. Pin output is set Low, so as to discharge the external capacitor. All the collected ADC data contain the discharge waveform of the external capacitor connected to the pin. They are screened to find when the measured voltage across the capacitor overcomes the threshold (adcData¿=41418). Note: the first 4 samples seem to be affected by noise, thus they are ignored. 63.2%(2î6= = 63.2%(65.536) = 41418.752

the time constant is computed (in msec) and used to obtain the capacitance value (in uF), which is then sent over UART (9600 baudrate) for visualization.

3.6 Firmware - Capacitance Measurement based on PSoC only

The Firmware of this thesis project has been developed inside the free Integrated Design Environment (IDE) that comes along with Cypress PSoC devices: 'PSoC Creator', which enables concurrent hardware and firmware editing, as well as compiling and debugging [32]. Featuring schematic capture and over 150 peripheral Components (e.g., analog and digital peripherals represented by a symbol), this software provides an easy way to configure and program the many analog- and digital-peripherals that are available on PSoC platform, to meet a variety of application requirements. With the aid of this intuitive software, the user can easily drag-and-drop components from the Cypress Component Catalog into the circuit design, connect them with the wiring tool and configure them through the graphical customizer dialog and a full set of dynamically generated API libraries. After configuring all the hardware peripherals, firmware can be written using C and/or Assembly programming

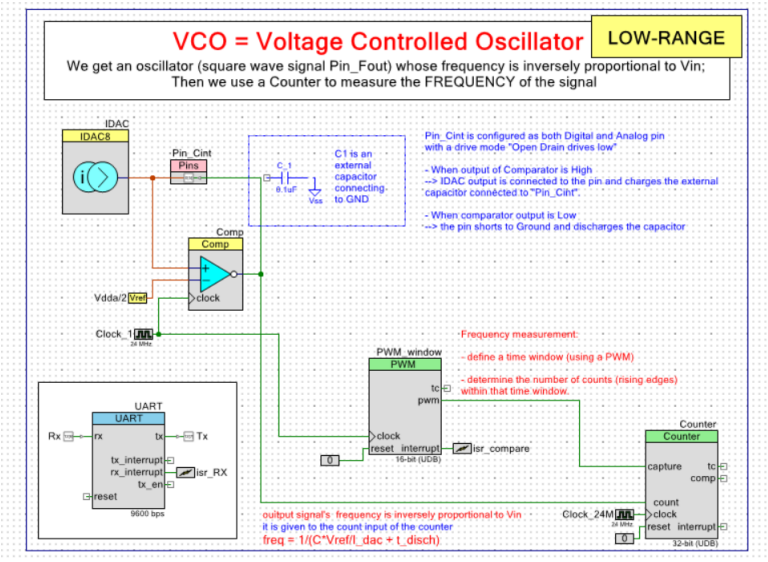

Figure 3.11: *PSoC Creator: Top Design showing PSoC peripheral components and their routing.*

language, with no code size limitations, and finally compiled, and debugged: all of this within PSoC Creator environment.

3.6.1 Top Design

3.6.1.1 Capacitance-Controlled Oscillator Circuit (CCO)

This first part of the circuit, showed in figure 3.12 is inspired by the Voltage-Controlled Oscillator (VCO) implemented by Cypress Community [33]. It exploits two of PSoC internal resources: IDAC and Comparator components. This circuit can be connected either to an external varying capacitor or to a capacitive sensor through pin 'Pin_Cint'.

The output of this circuit is a square wave whose frequency is controlled by three elements: the voltage applied at the inverting input of the comparator, the current supplied by the IDAC source, and the external capacitance at pin 'Pin_Cint'. However, In this application, both the voltage and the current are set constant, whereas the only value that is expected to change is that of the external capacitive sensor attached to the pin, which is represented in the Top Design as an unknown equivalent capacitor.

IDAC block is configured as a 100µA current source (see Table 3.6). Pin_Cint is configured as both Digital and Analog pin, with a drive mode 'Open Drain drives low' (figure 3.13), and it is internally routed both to the IDAC output and to the comparator's output. The comparator takes as inputs the voltage signal measured at Pin_Cint and the reference voltage threshold, which is set to Vdda/2 (e.g., 2.5V, since the PSoC is supplied with 5V Vdda). Comparator is set for inverted logic. hence, when the pin voltage overcomes the threshold voltage, its output turns low, and viceversa. Initially, when the output of the Comparator is High, the IDAC output is connected to the pin Pin_Cint, providing a 100 µA current to the external component, thus it charges the external capacitor.

When the Pin voltage crosses the threshold, which is set by the Vdda/2 voltage reference applied at the negative input of Comparator, the output of this component becomes low, shorting the pin to Ground and consequently discharging the capacitor. As capacitor voltage becomes zero, the Comparator output becomes high, the IDAC starts charging the capacitor again and the cycle is repeated: the result is a square wave, whose frequency contains infor-

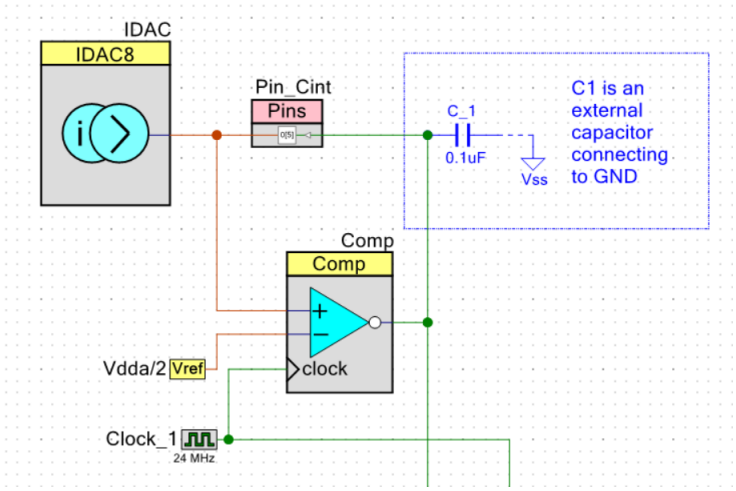

Figure 3.12: *Voltage-Controlled Circuit: PSoC components and their routing.*

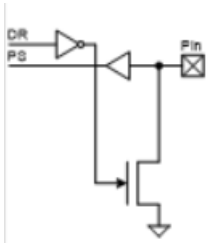

Figure 3.13: *Pin configured with drive mode: 'Open Drain - Drives Low'*

Value	100 µA
Polarity	Positive (Source)
Range	[0; 255] µA
Speed	High Speed

Table 3.6: *Configuration of IDAC Component:*

Polarity	Inverting
Hysteresis	Disabled
Speed	Fast
Sync	Normal
Clock	24 MHz
V_{ref}	2.5V (Vdda/2)

Table 3.7: *Configuration of the Comparator Component:*

mation about the unknown capacitance. The relationship between the output frequency of the oscillator and the input capacitance is given by the following equation:

$$f = \frac{1}{\frac{C \cdot V_{th}}{I_{DAC}} + T_{clock}}[Hz] \tag{3.3}$$

Where: f is the output frequency (measured in Hertz [Hz]), C is the external unknown capacitance(measured in Farad [F]), V_{th} is the threshold voltage of Comparator (measured in Volt [V]), I_{DAC} is the current provided by the IDAC module (measured in Ampere [A]), and T_{clock} is the Period of the Comparator's Synch clock (measured in seconds [s]). Since in this application the clock drives the comparator with a high frequency (24MHz), the term T_{clock} can be neglected. This leads to the simplified formula:

$$f = \frac{I_{DAC}}{C \cdot V_{th}}[Hz] \tag{3.4}$$

Showing that the output frequency is inversely proportional to the input capacitance. In order to extract the capacitance value, the previous equation can be inverted:

$$C = \frac{I_{DAC}}{f \cdot V_{th}}[F] \tag{3.5}$$

It is important to take into account that the period of the synchronizing clock that drives the comparator should be long enough to discharge the capacitor, thus the frequency has a superior limit:

- By choosing a clock frequency which is too high (short clock period), the capacitor may not discharge completely.
- With a clock frequency that is too low (long clock period), the term T_{clock} in the the denominator of the equation begins to dominate, thus reducing the linearity.

The value of the clock also depends on the value of the capacitance being sensed: higher value of capacitor requires a longer discharge time, thus it is necessary to have an idea of the range of measurable value, in order to set the clock and the PWM time window accordingly.

3.6.1.2 Frequency Counter

According to the *Merriam-Webster Dictionary*, 'frequency' is defined as: 'the number of times that a periodic function repeats the same sequence of values during a unit variation of the independent variable'. Hence, the frequency of a square wave signal can be measured by counting the number of rising edges that occur within one second. Operatively, we have to define a time window and count the number of rising edges within that time window.

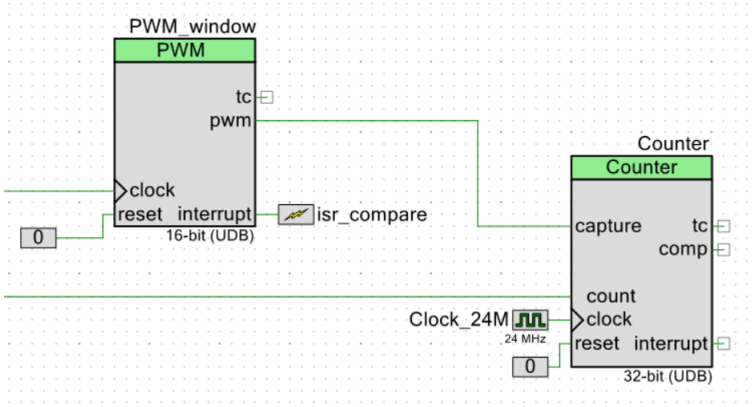

Figure 3.14: *Frequency Counter Circuit: PSoC components and their routing.*

$$f = \frac{counts}{TimeWindow}[Hz] \tag{3.6}$$

This part of the circuit (figure 3.14), devoted to the measurement of the frequency of the square wave produced by the CCO, uses a PWM and a Counter components [34].

The PWM Component (table 3.8) is used to generate, with its period, the time window: it is configured as to produce a square wave with a duty cycle of 50 percent and time period of 2.5 ms (thus a pulse width of 1.25ms) that becomes the 'capture signal' entering the Counter. The Counter (table 3.9) is driven by a 24MHz clock and by two inputs: 'capture' and 'compare': the signal whose frequency is to be measured (e.g., the square exiting the Comparator module in the CCO circuit) is routed to the 'count input' of the Counter, which is synchronized to the 24 MHz clock, in a way that it increments for every rising edge seen at its input; the 'capture input' role is to detect the starting and ending points of the time window generated by the PWM component, and to force a capture of the counts whenever a rising edge of the PWM occurs (the Counter's 'Capture Mode' is configured to be 'on Rising Edge'). When the rising edge of the PWM is detected, the counter captures the count value (which contains information about the input signal frequency) and resets for the next time window ('Reload Counter' is set to 'On Capture' and 'On Reset'). The counter is also reloaded on reset to prevent any false counts outside the time window. At the same moment in which the compare event occurs, an interrupt is generated in the PWM, sets a flag which is then polled in the main program and the calculation to extract the frequency info is performed (The frequency is calculated in Hz), thus we update the frequency every 2.5ms.

In the code of the Interrupt Service Routine (ISR) generated by a hardware signal from the PWM component, the PWM Status Register is read, in order to clear the Interrupt bit (it is important to do so because this bit is not cleared automatically, and otherwise the interrupt would run only once, and not occur continuously).

A proper capture occurs only when at least two rising edges in the Count input occur while the Capture input is high, which is during the 1.25 ms pulse of the PWM (the time window should have a period at least twice the one of the CCO signal to be measured): if this was limited to 1 rising edge, the asynchronous occurrence of the Capture input with respect to the Count input might result in missing the Capture signal. For this reason, the circuit is able to measure frequencies down to 800 Hz (period = 1.25 ms).

Resolution	16 bit
Period	2.5 ms
Duty Cycle	50%
Run Mode	Continuous
Interrupts	On TC and on Compare Event

Table 3.8: *Configuration of the PWM Temporal Window Component:*

Resolution	32 bit
Period	2^{32}-2
Compare value	255
Clock Mode	Up Counter
Run Mode	Continuous
Re-load Counter	on capture, on reset, on TC

Table 3.9: *Configuration of the Counter Component:*

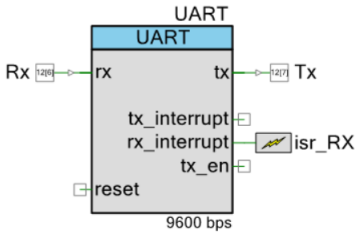

Figure 3.15: *Firmware (Top Design): UART module for Serial Communication with the GUI*

Baud Rate	9600 bps
Data bits	8
Parity Type	None
Stop bits	1
Flow Control	none

Table 3.10: *Configuration of the UART Component:*

3.6.1.3 UART

For transferring data from the PSoC to the GUI, a UART module was inserted in the Top Design (figure 3.15). The baud rate was set to 9600bps. An ISR ('Interrupt Service Routine') is triggered whe a Byte is received, in order to process eventual commands from the GUI on real time.

3.7 Software (Graphical User Interface)

The Graphical User Interface (GUI) has been developed using 'Processing', a free and open source software sketchbook based on Java programming language.

Menu Inside the initial Menu, user is asked to select the COM Port to be used for serial communication with the device, that should correspond to the port PSoC is using to send and receive data. One connection is established, the user can access three different pages: 'Calibration', 'Measurement' and 'Post-Calibration'.

TimeWindow	2.5 msec
Current	100.0 µA
V_{th}	2500.0 mV
C_{par}	36 pF

Table 3.11: *Table with the Algorithm settings:*

(a) Page Menu

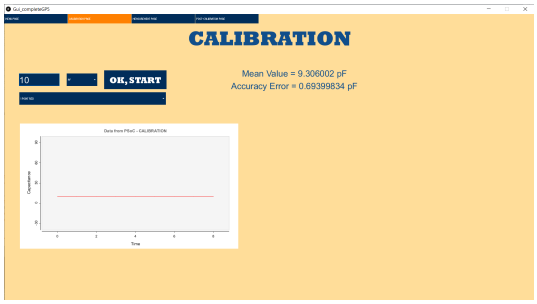

(b) Page Calibration

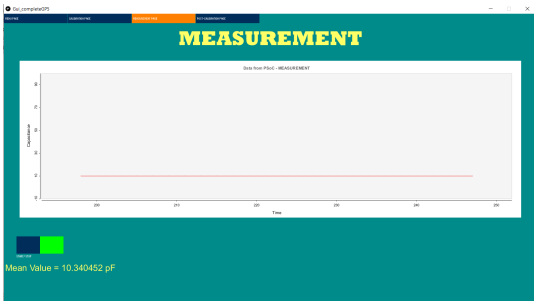

(c) Page Measurement

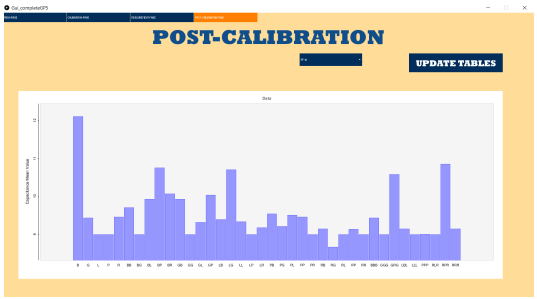

(d) Page Post-Calibration

Figure 3.16: *GUI: Graphical User Interface*

Calibration Calibration screen has been developed to be used for the initial tests performed on physical ceramic capacitors, aimed at comparing directly the value measured by the system against the 'True Value', of the capacitor under test (CUT) in order to determine the accuracy error on the output of the sensor. The user can insert manually the reference value of the capacitor under test (CUT) and then start a measurement: the measure is automatically repeated for 10 times and finally the mean value over the 10 collected values is computed.

Measurement The Measurement page provides the possibility to sample in real-time the valued of the capacitance/capacitive sensor attached to the device system, and plot those values on a temporal graph. Hence, this page was exploited during the measurement protocol explained in section regarding MIP-covered chip preparation procedure (see Table 4.2) in order to track the changes in capacitance over time of the device under different expositions to Toluene. Analogously to a digital oscilloscope, every time 10 consecutive samples are collected, the mean value is istantaneously computed and printed onto the screen, so that the user can visually chek the updated measured value. In the mean time, the values are registered on a txt file which is saved in the memory of the computer.

Post-Calibration In this page it is possible to see altogether the measurements that have been collected for a certain nominal value of capacitors, in order to visually check the variability of the capacitance value between different capacitors.

Chapter 4

Experimental Tests and Results

4.1 Calibration using ceramic capacitors

In the first phase of this work, the intended purpose was to characterize the sensor system by defining its accuracy applied to the measurement of capacitors of well known capacitance, in the pF range, since it is expected that, being the amount of Toluene present in human exhaled breath really low, and being the polymeric film devoted at molecular recognition extremely thin (i.e.: in the range of nanometers), the capacitance changes detected in the sensor in real application to exhaled breath will be either in the pF range, or even lower.
'Calibration' is an experimental procedure that, regardless the instrument's operating principle, constructs a curve point-by-point by using the samples of the input quantity (in this case, the capacitance), measured by a 'reference instrument', whose accuracy is known and is at least one order of magnitude higher than that of the instrument to be calibrated. In this thesis project, the reference sensor is the commercial IC FDC1004Q Capacitance-to-Digital Converter presented in the previous sections.
Having defined:
u = output of the 'reference instrument' (i.e.: the commercial Capacitance-to-Digital Converter).
u_x = output of the instrument that needs to be calibrated (i.e.: the PSoC-based system presented in this manuscript).
The calibration procedure works as it follows: as the intensity of the input quantity varies, we compute the difference $(u_x - u)$, which is the deviation between the measurement of the instrument under test and the reference.

- If $(u_x - u) < 0 \rightarrow u_x < u$: it means that the instrument under test (u_x) underestimates the input quantity, thus calibration requires positive correction, that is the addition of the deviation term: $u_x + (u - u_x)$
- If $(u_x - u) > 0 \rightarrow u_x > u$: it means that the instrument under test (u_x) overestimates the input quantity, thus calibration requires negative correction, that is implemented by subtracting the deviation term: $u_x - (u - u_x)$

We performed many measurements on a set of ceramic capacitors of seven different nominal values, ranging from a minimum of 10 pF to a maximum of 100pF, provided by a 'Bojack' kit. For each nominal value, 40 different pieces of the same fabrication stock were independently measured. Since every physical capacitor admits a certain tolerance on the effective value of the capacitance, we intended to validate the sensor'r response by means of the commercial

Nominal Value	Accuracy (absolute value)	Accuracy (% of true value)
10 pF	-1.130423786	-9.84%
20 pF	-1.897217351	-9.45%
30 pF	-2.589649815	-8.65%
47 pF	-1.373501268	-3.01%
56 pF	-1.886133143	-3.42%
68 pF	0.70903687	1.12%
100 pF	-0.108779688	-0.10%

Table 4.1: *Calibration of the capacitive PSoC-based sensor system, compared to the Capacitance-to-Digital Converter. Accuracy Error for different capacitors: expressed as absolute value or as a percentage with respect to the 'true value'.*

converter, considering the 'true value' being equal to the value of the capacitance effectively measured by this reference sensor.
In Table 4.1 are reported the nominal values of the capacitors under test, with the corresponding accuracy. The absolute value of accuracy was computed by the following way: for each one of the 7 nominal values, 40 distinct capacitors were available. For each element, 10 consecutive measurements are taken and immediately averaged, both with the PSoc-based system (by the 'Calibration' Page in the GUI) and with the Commerical I.C. CapConverter, so that the a set of 40 absolute values of accuracy error was computed:

$$AccuracyError_{absolute} = u_x - u \qquad [pF] \tag{4.1}$$

And the corresponding set of 40 accuracy errors expressed as a percentage value of the reference were calculated as:

$$AccuracyError_{\%} = \frac{u_x - u}{u} \cdot 100 \tag{4.2}$$

Then, the overall absolute accuracy value for a fixed nominal value was computed by averaging the 40 values, and the same for the computation of the percentage, which are both listed in Table 4.1.

4.2 Experimental Setup for Adsorption steps

At the end of the procedure of MIP preparation, described in the previous sections, several different chips are obtained, according to:

- the **state of the electrode**: either new IDAs or already used (that is, an electrode which has been already submitted to the deposition of the thin-film MIP and had been cleaned for further reuse).
- the **amount of MIP used to build the active layer**: in order to study how of the thickness of the polymeric film affects the response, deposition has been carried out with three different volumes (V1 = 4µL, V2 = 8µL, V3 = 12µL) of polymeric solution (i.e., the host-polymer combined with the Toluene template), so as to create differences in the MIP layer thickness.
- the **technique used for template removal**: to clear away the template from the polymer cavities by using an organic solvent (Acetone) or by evaporation inside the vacuum heater.

Acetone		*Vacuum*	
New	**Used**	**New**	**Used**
15 min: N-sol-V1-RA1	15 min: U-sol-V1-RA1	15 min: N-vac-V1-RA1	15 min: U-vac-V1-RA1
30 min: N-sol-V1-RA2	30 min: U-sol-V1-RA2	30 min: N-vac-V1-RA2	30 min: U-vac-V1-RA2
60 min: N-sol-V1-RA3	60 min: U-sol-V1-RA3	60 min: N-vac-V1-RA3	60 min: U-vac-V1-RA3
120 min: N-sol-V1-RA4	120 min: U-sol-V1-RA4	120 min: N-vac-V1-RA4	120 min: U-vac-V1-RA4
15 min: N-sol-V2-RA1	15 min: U-sol-V2-RA1	15 min: N-vac-V2-RA1	15 min: U-vac-V2-RA1
30 min: N-sol-V2-RA2	30 min: U-sol-V2-RA2	30 min: N-vac-V2-RA2	30 min: U-vac-V2-RA2
60 min: N-sol-V2-RA3	60 min: U-sol-V2-RA3	60 min: N-vac-V2-RA3	60 min: U-vac-V2-RA3
120 min: N-sol-V2-RA4	120 min: U-sol-V2-RA4	120 min: N-vac-V2-RA4	120 min: U-vac-V2-RA4
15 min: N-sol-V3-RA1	15 min: U-sol-V3-RA1	15 min: N-vac-V3-RA1	15 min: U-vac-V3-RA1
30 min: N-sol-V3-RA2	30 min: U-sol-V3-RA2	30 min: N-vac-V3-RA2	30 min: U-vac-V3-RA2
60 min: N-sol-V3-RA3	60 min: U-sol-V3-RA3	60 min: N-vac-V3-RA3	60 min: U-vac-V3-RA3
120 min: N-sol-V3-RA4	120 min: U-sol-V3-RA4	120 min: N-vac-V3-RA4	120 min: U-vac-V3-RA4

Table 4.2: *Re-adsorbing MIPs: Experimental Protocol for MIP-sensor exposition to Toluene*

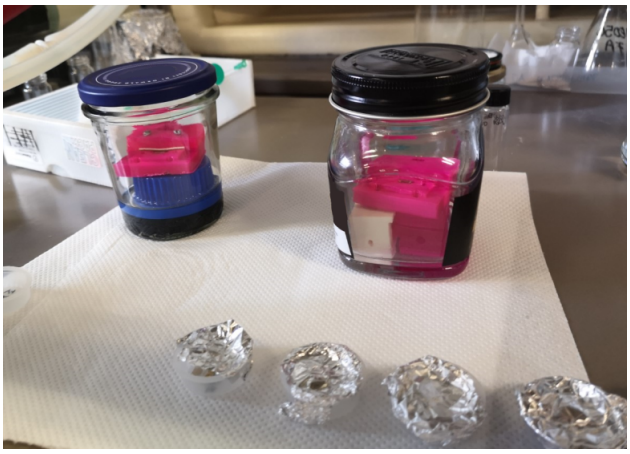

Figure 4.1: *SetUp for Adsorption Measurements: The sensors, mounted onto the open plastic support, are inserted into Glass Chambers that have beed saturated by Toluene (i.e.: a certain amount of liquid Toluene is still present at the bottom of the containers).*

N	chip was New
U	chip was already Used
sol	Toluene removed by Acetone Solvent
vac	Toluene removed by Vacuum (in the Heater)
V1	a volume of 4 uL polymeric solution was deposited
V2	a volume of 8 uL polymeric solution was deposited
V3	a volume of 12 uL polymeric solution was deposited
RA1	chip was exposed to Toluene for 15 min
RA2	chip was exposed to Toluene for 30 min
RA3	chip was exposed to Toluene for 60 min
RA4	chip was exposed to Toluene for 120 min

Table 4.3: *Re-adsorbing MIPs: Legenda*

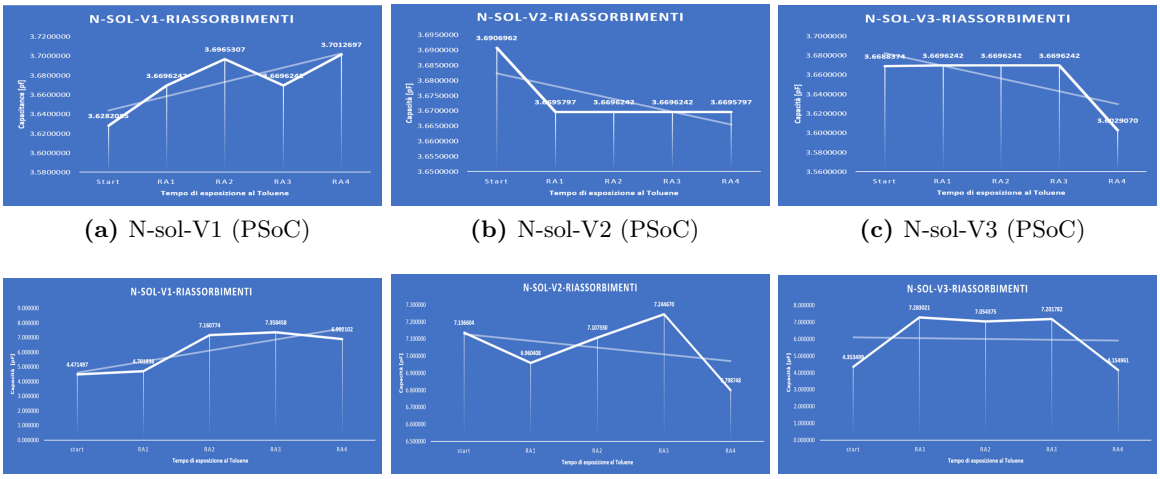

(a) N-sol-V1 (PSoC) **(b)** N-sol-V2 (PSoC) **(c)** N-sol-V3 (PSoC)

(d) N-sol-V1 (CapConverter) **(e)** N-sol-V2 (CapConverter) **(f)** N-sol-V3 (CapConverter)

Figure 4.2: *Effect of Re-adsorption of Toluene on sensors cleaned with solvent: absolute value of Capacitance (PSoC vs CapConverter)*

After creating the several different sensors, by varying the amount of deposited polymer and the method used for template removal, as illustrated in the previous chapter, we submitted each sensor to a series of adsorption steps, during which the chip was closed inside a Toluene saturated chamber, in static conditions. The aim of this experimental protocol was to investigate how Toluene is adsorbed by the sensor when exposed to a great amount of this molecule for increasing time intervals, consisting of 15, 30, 60 and 120 minutes, while characterizing its electrical response. Saturated environment inside the adsorption cell was reached by introducing, by means of a micropipette, 30 mL of liquid-phase Toluene inside the glass chamber, since this volatile compound is purchased in liquid phase, but it evaporates easily at room temperature. Then, the plastic support, containing the sensor under test, was introduced in the adsorption cell, and hermetically sealed, being careful not to put the liquid in contact with the PLA material so to prevent any damage to the structure.
Table 4.2 illustrates the breakdown of the different sensors submitted to the adsorption experimental procedure. The increasing adsorption time intervals, consisting of 15, 30, 60 and 120 minutes, were labeled, respectively: RA1, RA2, RA3, RA4 (those labels stand for 'Re-Adsorption number 1, 2, 3 and 4).
Capacitive measurements have been collected from both the customized PSoC-based sensor system and the commercial Capacitance-to-Digital Converter FDC1004Q, (here, for convenience, referred to as 'CapConverter'), and at the end of the overall experimental procedure we resumed all the data by plotting them separately.
Against all our positive expectations, the responses, with both systems, appear quite unstable, showing fluctuations that are difficult to relate to the increased exposition interval to Toluene. In particular, for the PSoC-based system, the measured capacitance variations between the different phases are so low that they might be attributable to measurement errors or disturbances, rather than to a useful capacitive signal cased by introduction of Toluene inside the dielectric's cavities.

4.2.1 Re-Adsorption Steps: template removed with Acetone Solvent

However, by tracking the capacitance value measured by the PSoC-based device and the CapConverter along the different steps of adsorptions, it has been found that, **for the chips that were cleaned with Acetone solvent**:

- N-sol-V1: for the new (N) electrodes with the thinnest MIP layer (volume V1), the C shows an overall positive trend in both the PSoC-based and the CapConverter systems.
- N-sol-V2: for the new electrodes with the intermediate MIP film thickness (volume V2), the overall trend is negative, in both the PSoC-based and the CapConverter systems.
- N-sol-V3: for the new electrodes with the thickest layer (volume V3) the measurements with the the PSoC-based system seem to be wasted, since they give exactly the same identical output value for re-adsorptions steps RA1, RA2 and RA3, by showing a slight decrease after the last adsorption interval. Differently, in the capConverter, the overall trend is flat, since the capacitance results increased by almost 3 pF after the first adsorption steps, and then it mantains itself almost equal for the successive two adsorption steps, finally going downwards to meet a value of C slightly inferior to the one of the starting chip.

Delta Capacitance During the measurement protool, we noticed that the system's offset capacitance (i.e. the base signal, or the output value corresponding to an open circuit measurement) was changing, maybe influenced by the Laboratory environmental conditions (measurements were performed in the second middle of July). Hence, by observing the change in capacitance in the CapConverter, with respect to the base signal measured immediately before the measurement (the deltaC), it has been found:

- N-sol-V1: the new electrodes deposited with volume V1, the trend is decreasing with adsorbtion time, meaning that the capactance always increases after exposition to toluene, but that the entity of this increase is higher after RA1 than after RA4. It could be inferred that when the mip is cleaned, a large amoun of toluene is trapped inside its cavities, thus producing a satisfacotry increase in the sensor's capacitance, but also making it more difficult to adsorb new toluene molecules, thus the variation of capacitance registered becomes lower beacause the entity of asorption of the mip becomes less effective with expositon time.
- N-sol-V2: for the new (N) electrodes with the intermediate volume V2, the trend is slightly positive, but the deltaC value after the second re-adsorption step RA2 shows the lower value: 0.98pF, whereas the maximum value is correspondent to the RA3 (1.58pF)
- N-sol-V3: for the new electrodes produced by V3, the general trend is also positive, but again the maximum value is in correspondence of the RA3 (1.3 pF)-

4.2.2 Re-Adsorption Steps: template removed inside the Vacuum Heater

For the chips that were **cleaned inside the vacuum heater**: for the new (N) electrodes, regardless the thickness of the MIP layer (so it is the same for V1, V2 and V3) the trend measured with the PSoC-based system is always slightly negative, but it has been discarded since it is considerered poorly informative. Conversely, the behaviour registered by the CapConverter is the different: the trend is slightly increasing for the first 2 volumes V1 and V2, then for the thickest layer V3 it is almost flat.

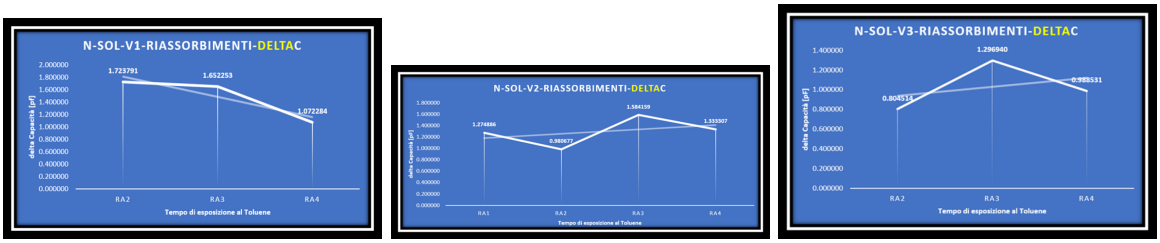

(a) N-sol-V1 (CapConverter) **(b)** N-sol-V2 (CapConverter) **(c)** N-sol-V3 (CapConverter)

Figure 4.3: *Effect of Re-adsorption of Toluene on sensors cleaned by Solvent: delta of Capacitance (CapConverter)*

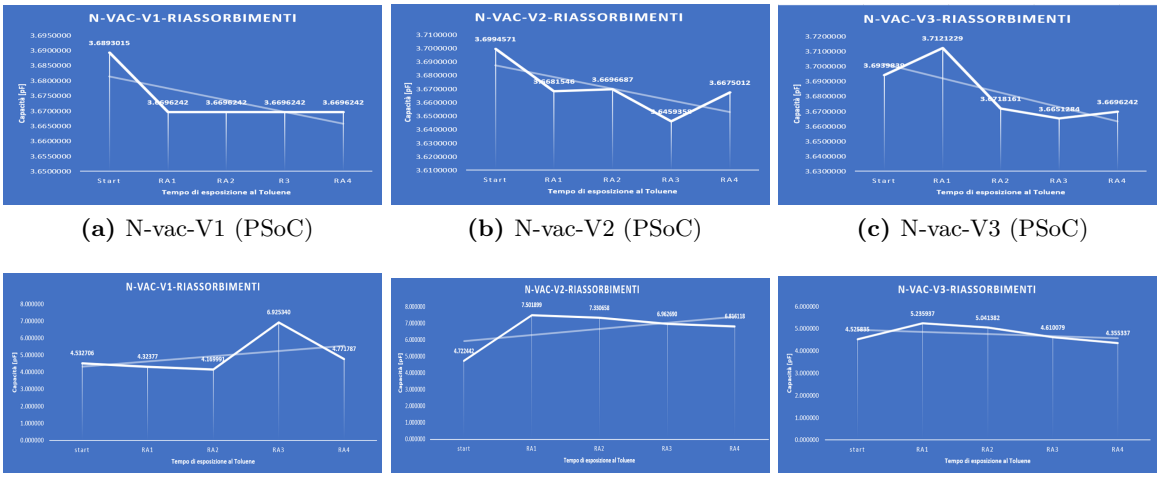

(a) N-vac-V1 (PSoC) **(b)** N-vac-V2 (PSoC) **(c)** N-vac-V3 (PSoC)

(d) N-vac-V1 (CapConverter) **(e)** N-vac-V2 (CapConverter) **(f)** N-vac-V3 (CapConverter)

Figure 4.4: *Effect of Re-adsorption of Toluene on sensors cleaned inside the Vacuum Heater: absolute value of Capacitance (PSoC vs CapConverter)*

- For N-vac-V1: The Cap Converter measured lower and lower values from the starting unexposed sensor (4.53 pF), up to the first two re-adsorption phases, then capacitance increased by almost 3pF after the third phase, concenring 1 hour of exposition to the saturated environment, and then a decrease to a value of 4.77pF, similar to the one of the unexposed chip.
- For N-vac-V2: in this case the measured quantity reched a peak of 7.50 pF right after the first exposition phase, and then a slow decrease for the next adsorption steps, until a 6.81 pF for the fourth step RA4.
- For N-vac-V3: this graph is similar to the previous one, except that the overall capacitance variation shows a a narrower range. from the initial value of 4.53 pF prior any exposition, to a peak of 5.24 pF after RA1, and then a slow decreease during the following adsorption steps RA2, RA3, and RA4, correspondig to 5.04 pF, 4.61 pF, and 4.36 pF respectively.

4.2.3 Effect of MIP-thickness: New vs. Used Electrodes

This analysis was applied only to the electrodes that have been cleaned by the use of the solvent, thus the comparison is between New and Used IDAs. Figure 4.5 shows four plots:

the two upper plots correspond to the outcome recordered for New (N) electrodes, both with the PSoC-base device (on the left) and with the CapConverter, whereas the two graphs on the bottom are related to the Used IDAs. The capacitance outcome of each device is plotted in pF unit, for different conditions of the electrodes: 'plain' indicates the un-treated electrode, without any polymeric layer and prior any cleaning procedure with water and ethanol, then measurement is taken for the electrodes after cleaning (U1 and N1), and after functionalization of their surface with BODS (U2, N2), so that we can see the effects on sensor capacitance along the different steps of preparation that precedes the MIP deposition. After that, values are plotted for the three deposition volumes V1, V2 and V3, so as to check what is the correlation between the thickness of the polymeric layer and the outcome of the two measurement systems. Those values are intended to be the capacitance 'baseline' value, hence only after MIP volumes deposition, polymerization and template removal by acetone, but prior any rebinding to toluene in the adsorption chamber.
Unfortunately, because of lack of time, we did not test the re-adsorption on Used electrodes. By analyzing the response of the CapConverter for the different deposition steps, we can infer that:

- for the New Electrodes: we can see that the 'plain' electrode, which is measured prior cleaning, shows a capacitance value of 4.61 pF, then after cleaning with water and ethanol the measured C is increased up tu 6.91pF, after unctionalization it is decreased again to a value slightly higher than the initial one (4.79pF). Then, for the sensors that have been created with volumes V1 and V3, the capacitance baseline value (prior any rebinding to toluene in the adsorption chamber) is surprisingly very similar, being respectively 4.47 pF and 4.35 pF Instead, the sensor with intermediate MIP thinckness shows a much greater value (7.14 pF).

- for the Used electrodes: the C value measured before and after the cleaning procedure seems almost unchanged (4.61 and 4.56 pF), whereas there is a considerable peak after functionalization (chip U2) when the capacitance is almost doubled (8.32 pF) with respect to the initial values. After deposition of the polymer layer, the output registered values are again low, showing a decrease with the increment of MIP used to build the film (5.1, 4.48, 4.44 pF are recorded ro respectively, V1, V2, and V3).

4.2.4 Measurement of Resistance

Beyond the capacitive sensing, some resistive measurements have been conducted on the sensors as well, at the interval between each of the aforementioned steps. Like the proposed capacitive system, also the resistance measurement has been implemented based exclusively on internal resources of the PSoC.
Being the Toluene-imprinted polymer a dielectric material, since it has not been doped with any conductive material, it was expected to found a very high value of electrical resistance.
Indeed, as expected, the resistance values were so high that they exceeded the measurement range admitted by the resistance-meter firmware, being confused with an open circuit condition.

4.3 Results

Unfortunately, the obtained results have not met the expectations.
Since the sensors were closed in an environment saturated with Toluene, we expected the maximum possible absorption from the MIP, with the consequent recording of the maximum

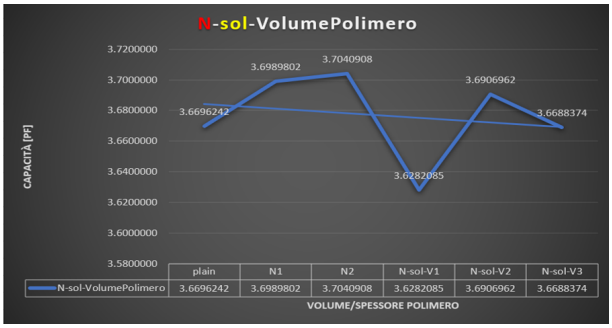

(a) N-sol-V (PSoC)

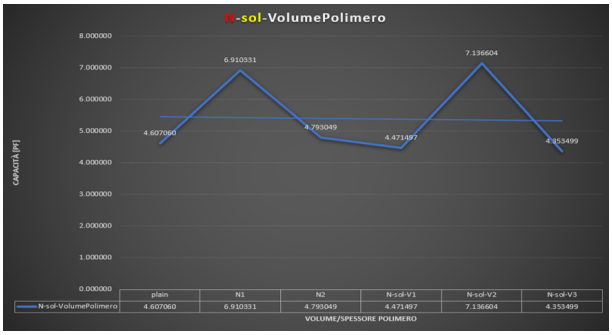

(b) N-sol-V (CapConverter)

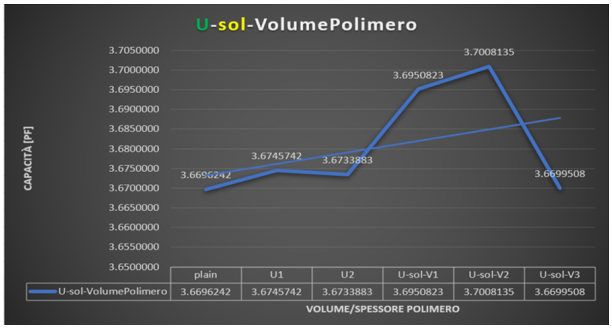

(c) U-sol-V (PSoC)

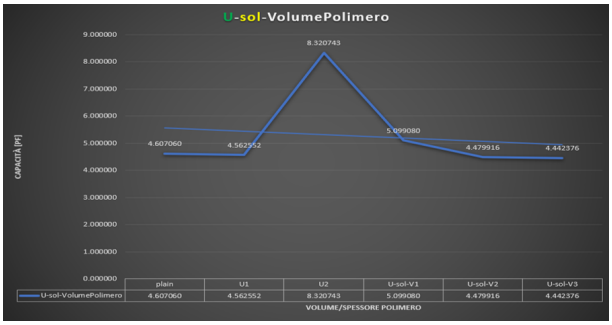

(d) U-sol-V (CapConverter)

Figure 4.5: *Effect of MIP-thickness (volume of deposited MIP): New vs. Used Electrodes.*

capacity deviation from the baseline.
Against all our positive expectations, the responses, with both systems, appear quite unstable, showing fluctuations that are difficult to relate to the increased exposition interval to Toluene.
In particular, for the PSoC-based system, the measured capacitance variations between the different phases are so low that they might be attributable to measurement errors or disturbances, rather than to a useful capacitive signal cased by introduction of Toluene inside the dielectric's cavities.
It may be inferred that the capacitance variation in the developed polymer-based sensor are so low that the proposed measurement system is not able to capture them.

Chapter 5

Conclusive Discussion and Future Research Development

As part of the research for new techniques aimed at achieving an early diagnosis of lung cancer, this thesis project was aimed at developing a sensor system capable of measuring the concentration of Toluene in gas mixtures, as this compound appears to be a promising candidate for the role of biomarker for the target disease.
The proposed chemical sensor is composed by a gold Interdigitated Electrode Array (IDA), with a planar circular pattern, coupled to a thin film of Toluene-Imprinted Polymer (MIP), which is the active material, thus aimed at molecule recognition.
Being the MIP is an insulating material deposited onto the interdigitated array, hence interposed between the microelectrode strips, the sensor's electrical capacitance is the addressed variable, that should be dependent on the properties of the dielectric MIP in between the interdigitated fingers. Hence, some kind of variation in the sensor's overall capacitance is expected to be recorded, once the chip is exposed to a gas mixture containing Toluene.
Two methods for capacitive sensing have been tested throughout this work, both entirely based on the on-chip resources present in the PSoC development kit.

The first sensing technique, relying on the **computation of the time constant of an RC circuit** in which the capacitance is the unknown sensor value to be extracted, was unable to measure capacitors lower than the micro-Farad range, because it relies on the sampling of the external capacitor's charging process while it is being charged to a known voltage, thus requiring accurate detection of the instant corresponding to the circuit's time constant. However, this solution gave poor results already with capacitors equal or lower than 100 nF. Thus, the method based on the computation of the time constant is not employable to the target task, in which low range of capacitive variations are expected to be found. Since this system relies on a a minute IDA electrode based on a thin layer of adsorbing material (the thin-film MIP, whose thockness is in the range of nanometers), specially from the moment that the final application of such kind of devices is expected to be targeting rare traces of Toluene in a more complex mixture (i.e., the human's exhaled breath) in presence of many other similar volatile compounds.

Thus, the first readout electronics was soon discarded, in favor of the second method: **the final developed system** relies on a circuit realized exclusively within the PSoC, consisting of a **capacitance-controlled oscillator (CCO)**, aimed at the conversion from the value of the external sensors's capacitance into a square wave, whose frequency carries the information

about the input variable, coupled to a **frequency counter** circuit. By adjusting the time window used to measure the square wave generated by the CCO circuit (in this case, with a time window of 2.5 ms), it is possible to measure with sufficient accuracy capacitors in the pF range.

By comparing the developed PSoC-based sensing system with the miniaturized commercial FDC1004Q Capacitance-to-Digital Converter, it showed satisfying accuracy within the range from 10 to 100 pF, even though not being constant all over the range.
In fact, the percentage accuracy error, with respect to the reference value provided by the FDC1004Q, tends to be higher close to the bottom of the measuring range, for example, being the absolute accuracy error of -1.13 when applied to a capacitor close to 10 pF, the percentage error was -9.83%, whereas this percentage accuracy error results to be extremely low -0.10% for the 100 pF capacitors.

Finally, both the PSoC-based system and the I.C. Capacitance-to-Digital Converter have been effectively tested for Toluene detection, in order to evaluate the capacitive response of the developed MIP-based sensor through a series of adsorption phases within a saturated chamber, at room temperature.
Since the sensors were closed in an environment saturated with Toluene, it was expected to reach the saturation of the MIP (that is, the maximum possible absorption capability is given by the cavities that are available for rebinding), with the consequent recording of the maximum capacity deviation from the baseline. The measuring protocol adopted in this thesis project involved the use of an environment saturated with Toluene vapor, because the first task was to understand whether the developed sensor was actually able to detect the presence of the target, at least when the latter was present at its maximum concentration, hence in the easier possible condition.
Unfortunately, the results are not satisfactory: against all the positive expectations, the responses that have been recorded with both systems after each of the four adsorption steps, appear quite unstable, showing fluctuations that are difficult to relate to the increased exposition interval to Toluene.
Moreover, it was impossible to highlight a linear response between the sensor exposition time to Toluene and the measured capacitance, neither with the PSoC data nor with the commercial CapConverter.
In particular, for the PSoC-based system, the measured capacitance variations between the different phases are so low that they might be attributable to measurement errors or disturbances, rather than to a useful capacitive signal cased by introduction of Toluene inside the dielectric's cavities. Hence, it may be inferred that the capacitance variation in the developed polymer-based sensor are so low that the proposed measurement system is not able to capture them.
Beyond the capacitive sensing, some **resistive measurements** have been conducted on the sensors as well, at the interval between each of the aforementioned steps, with the only aim to confirm the dielectric nature of the thin polymer layer. Similarly to the proposed capacitive system, the resistance measurement has also been implemented based only on internal resources of the PSoC. Being the toluene-imprinted polymer a dielectric material, it was expected to found a very high value of electrical resistance. Indeed, as expected, the resistance values were so high that they exceeded the measurement range admitted by the resistance-meter firmware, that is 940 kΩ, being confused with an open circuit condition.
Unfortunately, the final goal, consisting in the the development of a selective and extremely accurate sensor for the detection of Toluene is still very far from this point, since there is

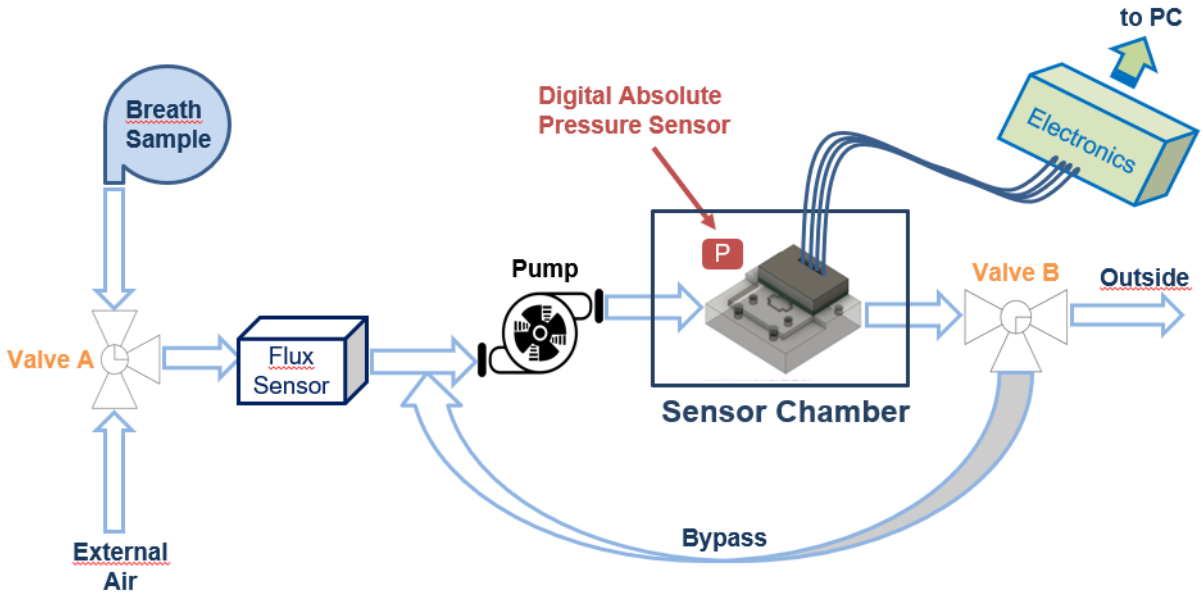

Figure 5.1: *An example of gas circuit that could be used for further analysis on exhaled breath bag samples.*

still the need to perform a massive number of measurement, so as to improve the resolution of the device so as to be able to catch the minimal differences and be applied to dynamic measurements on real samples from human breath.
Indeed, the successive step is to improve the here presented capacitive sensing system, by validating its results on a wider range, trying to catch smaller capacitance variations and separate them by any disturbances.
A further improvement would be pursuited by testing other kind of measurements, such as the resistance or impedance sensing, by introducing small amounts of conductive nanomaterials inside the formulation of the MIP: for example, as it can be found in literature regarding polymer-based chemiresistors, Gold Nanoparticles or Carbon Nanotubes can be used for this purpose.

The final achievement would be to finally test the proposed Toluene sensor to real samples collected in the human breath, so as to understand if it is able to selectively bind the target molecule even if in the adverse condition in which the target molecule is present at PPB concentrations in a more complex gaseous mixture comprehending many similar volatile compounds.
An example of an automated embedded system able to pursuit this goal is presented in figure 5.1. In such a system, MIP's micro-cavities should be 'cleaned' by passing a Nitrogen flow prior any measurement, so as to keep trace of the sensor'output corresponding to the measures the baseline C_o. Right after the cleaning nitrogen flux, the analysis could be performed, with the exhaled breath contained inside the Tedlar bag passing through the gas circuit, while the electronic circuit is monitoring the capacitance variation in the sensor.
In conclusion, there is still a lot of work that separates us from the final goal of obtaining new portable, highly accurate and selective MIP and IDA-based sensors for measurement of Toluene, that could be applied in a more advanced instrument for measuring VOCs pattern in exhaled breath in order to diagnose lung cancer at early stages.

Bibliography

[1] Ana María Casas-Ferreira, Miguel del Nogal-Sánchez, José Luis Pérez-Pavén, and Bernardo Moreno-Cordero. Non-separative mass spectrometry methods for non-invasive medical diagnostics based on volatile organic compounds: A review. *Analytica Chimica Acta*, 1045:10 – 22, 2019.

[2] Davide Marzorati, Luca Mainardi, Giulia Sedda, Roberto Gasparri, Lorenzo Spaggiari, and Pietro Cerveri. A review of exhaled breath: a key role in lung cancer diagnosis. *Journal of Breath Research*, 13(3):034001, 2019.

[3] Z. Jia, A. Patra, V.K. Kutty, and T. Venkatesan. Critical review of volatile organic compound analysis in breath and in vitro cell culture for detection of lung cancer. *Metabolites*, 9(3):52, 2019.

[4] Wouter H. van Geffen, Kevin Lamote, Adrien Costantini, Lizza E.L. Hendriks, Najib M. Rahman, Torsten G. Blum, and Jan van Meerbeeck. The electronic nose: emerging biomarkers in lung cancer diagnostics. *Breathe*, 15(4):e135–e141, 2019.

[5] Zi-Ao Zhou, Jiemin ans Huang, Ujendra Kumar, and David D.Y. Chen. Review of recent developments in determining volatile organic compounds in exhaled breath as biomarkers for lung cancer diagnosis. *Analytica Chimica Acta*, 996:1 – 9, 2017.

[6] S. X. Antoniou, E. Gaude, M. Ruparel, M. P. van der Schee, S. M. Janes, and R. C. Rintoul. The potential of breath analysis to improve outcome for patients with lung cancer. *Journal of Breath Research*, 13(3):034002, 2019.

[7] Ji-Eun Chang, Dae-Sik Lee, Sang-Woo Ban, Jaeho Oh, Moon Youn Jung, Seung-Hwan Kim, SungJoon Park, Krishna Persaud, and Sanghoon Jheon. Analysis of volatile organic compounds in exhaled breath for lung cancer diagnosis using a sensor system. *Sensors and Actuators B: Chemical: international journal devoted to research and development of physical and chemical transducers*, 2017.

[8] Serasanambati M., Broza Y.Y., Marmur A., and Haick H. Profiling single cancer cells with volatolomics approach. *iScience*, 11:178–188, 2019.

[9] Michael Phillips. Method for the collection and assay of volatile organic compounds in breath. *Analytical Biochemistry*, 247(2):272 – 278, 1997.

[10] Michael Phillips, Kevin Gleeson, J Michael B Hughes, Joel Greenberg, Renee N Cataneo, Leigh Baker, and W Patrick McVay. Volatile organic compounds in breath as markers of lung cancer: a cross-sectional study. *The Lancet*, 353(9168):1930 – 1933, 1999.

[11] Michael McCulloch, Tadeusz Jezierski, Michael Broffman, Alan Hubbard, Kirk Turner, and Teresa Janecki. Diagnostic accuracy of canine scent detection in early- and late-stage lung and breast cancers. *Integrative Cancer Therapies*, 5(1):30–39, 2006. PMID: 16484712.

[12] Annette G. Dent, Tom G. Sutedja, and Paul V. Zimmerman. Exhaled breath analysis for lung cancer. *Journal of thoracic disease*, 5 Suppl 5(Suppl 5):S540–50, 2013.

[13] B de Lacy Costello, A Amann, H Al-Kateb, C Flynn, W Filipiak, T Khalid, D Osborne, and N M Ratcliffe. A review of the volatiles from the healthy human body. *Journal of Breath Research*, 8(1):014001, 2014.

[14] Himanshu K. Patel. *The Electronic Nose: Artificial Olfaction Technology*. Biological and Medical Physics, Biomedical Engineering. Springer India, 1 edition, 2014.

[15] Sharina Kort, Marjolein Brusse-Keizer, Jan-Willem Gerritsen, and Job van der Palen. Data analysis of electronic nose technology in lung cancer: generating prediction models by means of aethena. *Journal of Breath Research*, 11(2), 2017.

[16] Joseph J. BelBruno. Molecularly imprinted polymers. *Chemical Reviews*, 119(1):94–119, 2019.

[17] Saylan Y., Yilmaz F., Özgür E., Derazshamshir A., Yavuz H., and Denizli A. Molecular imprinting of macromolecules for sensor applications. *Sensors*, 17(4):898, 2017.

[18] Saylan Y., Akgönüllü S., Yavuz H., Ünal S., and A. Denizli. Molecularly imprinted polymer based sensors for medical applications. *Sensors (Switzerland)*, 19(6), 2019.

[19] Claudio Baggiani, Cristina Giovannoli, Laura Anfossi, Cinzia Passini, Patrizia Baravalle, and Gianfranco Giraudi. A connection between the binding properties of imprinted and nonimprinted polymers: A change of perspective in molecular imprinting. *Journal of the American Chemical Society*, 134, 2012.

[20] William Henri Grover. Interdigitated array electrode sensors: Their design, efficiency, and applications. Honors thesis projects, University of Tennessee, 1999. Chancellor's Honors Program Projects.

[21] Micrux Technologies. *Thin-film InterDigitated Electrodes*.

[22] David Wang. *FDC1004: Basics of Capacitive Sensing and Applications*. Texas Instruments, December 2014. Application Report SNOA927-December 2014.

[23] David Wang. *Capacitive Sensing: Ins and Outs of Active Shielding*. Texas Instruments, February 2015. Application Report SNOA926A-February 2015-Revised February 2015.

[24] Texas Instruments. *FDC1004Q 4-Channel Capacitance-to-Digital Converter for Capacitive Sensing Solutions*, April 2015. SNOSCZ4-APRIL 2015.

[25] A. Aasi, S. M. Aghaei, and B. Panchapakesan. A density functional theory study on the interaction of toluene with transition metal decorated carbon nanotubes: a promising platform for early detection of lung cancer from human breath. *Nanotechnology*, 31, 2020.

[26] Xiaohu Ding, Dawen Zeng, Shunping Zhang, and Changsheng Xie. C-doped wo3 microtubes assembled by nanoparticles with ultrahigh sensitivity to toluene at low operating temperature. *Sensors and Actuators B: Chemical*, 155(1):86 – 92, 2011.

[27] Nam-Hoon Kim, Seon-Jin Choi, Dae-Jin Yang, Jihyun Bae, Jongjin Park, and Il-Doo Kim. Highly sensitive and selective hydrogen sulfide and toluene sensors using pd functionalized wo3 nanofibers for potential diagnosis of halitosis and lung cancer. *Sensors and Actuators B: Chemical*, 193:574 – 581, 2014.

[28] Amel Bajtarevic, Clemens Ager, Martin Pienz, Martin Klieber, Konrad Schwarz, Magdalena Ligor, Tomasz Ligor, and Tomasz Ligor. Noninvasive detection of lung cancer by analysis of exhaled breath. *BMC Cancer*, 9(1), 2009.

[29] Kim DG van de Kant, Linda JTM van der Sande, Quirijn Jöbsis, Onno CP van Schayck, and Edward Dompeling. Clinical use of exhaled volatile organic compounds in pulmonary diseases: a systematic review. *Respiratory Research*, 13(117), 2012.

[30] Geoffrey Gregis, SÃ©bastien Schaefer, Jean-Baptiste Sanchez, Vanessa Fierro, Franck Berger, Igor Bezverkhyy, Guy Weber, Jean-Pierre Bellat, and Alain Celzard. Characterization of materials toward toluene traces detection for air quality monitoring and lung cancer diagnosis. *Materials Chemistry and Physics*, 192:374 – 382, 2017.

[31] Cypress Semiconductor Corporation. *PSoC ® 5LP: CY8C58LP Family.*

[32] Cypress Semiconductor Corporation. *PSoC ® Creator ™ User Guide.* Document # 001-93417 Rev *K.

[33] Cypress Semiconductor Corporation. *Voltage Controlled Oscillator in PSoC ® 3 / PSoC 5.* docID=33522.

[34] Cypress Semiconductor Corporation. *Frequency Measurement With Counter in PSoC ® 3 / PSoC 5.*

Ringraziamenti

A conclusione di questo elaborato di Tesi Magistrale, vorrei dedicare qualche riga per menzionare tutti coloro che hanno contribuito alla sua realizzazione, sia direttamente che indirettamente.
Vorrei innanzitutto ringraziare il mio relatore, il Professor **Pietro Cerveri**, per avermi indirizzato verso questo fantastico progetto e per aver sempre cercato di tenere attivo il mio entusiasmo verso di esso.
Ringrazio infinitamente il mio correlatore e tutor **Davide Marzorati**, per la sua paziente disponibilitá, e per tutti gli spunti che è stato di darmi lungo questo percorso, per avermi guidato e aiutato.
Ringrazio i nostri collaboratori del dipartimento di Chimica: il **Professor Cellesi**, **Maria Isabel Martinez Espinoza** e **Marco Maroni**, che si sono occupati della realizzazione del MIP per il riconoscimento del Toluene, un elemento essenziale in questo lavoro.
Ringrazio i miei genitori, **Carlo** e **Daniela**, senza i quali non avrei mai raggiunto tale risultato, che mi hanno accettato e motivato, dandomi il coraggio di intraprendere una carriera che, senza il loro supporto totale, non avrei mai pensato di poter rendere mia. Ringrazio anche **Alessandro** e **Camilla**, per aver sempre creduto in me.
Ringrazio i miei amici di Roma, che rappresentano per me un appiglio importante e costante fonte di sicurezza e accoglienza, e che hanno contribuito prima di tutti alla mia crescita personale, ponendo quindi le basi per i miei progressi futuri. Innanzitutto, le mie care compagne dei tempi di triennale: **Maria Vittoria**, sempre cosí dolcemente protettiva e saggia, **Claudia**, che è sempre stata tenera nei miei confronti, e per me rappresenta un appiglio, **Federica**, tremendamente affettuosa e coinvolgente, e **Cecilia**, la quale, sebbene distante, rimane sempre nei miei pensieri.
Un pensiero va anche ai miei amici storici del liceo: **Junxiang**, il mio piú caro e geniale amico, **Gianluca**, compagno di squilibri mentali, **Davide**, che rimarrá sempre il mio saggio sensei, **Janica**, il cui brio mi coinvolge, rendendomi leggera, e **Giorgio**, amico dall'ironia fuori dal comune. E le amiche di sempre: **Janette**, sei la persona che conosco da piú tempo, durante questi tredici anni ci siamo perse e poi ritrovate, piú forti di prima, e ti sono estremamente grata. **Samantha**, abbiamo condiviso momenti duri della nostra vita, e ci siamo tenute compagnia in quelli piú lieti, sono contenta di essere tua amica.
Ringrazio i miei compagni di avventure qui a Milano, che mi hanno accompagnato in questi ultimi anni, aiutandomi a vivere e scoprire una cittá della quale ormai sono innamorata. Innanzitutto, le mie prime coinquiline, nonché amiche, **Teresa** e **Lucia**: insieme ci siamo divertite e siamo rimaste in contatto vivendo ogni angolo di questa dinamica cittá. Poi i miei attuali compagni di casa: **Chiara, Magda, Leonardo** e **Matilde**. Assieme a voi ho sperimentato la gioia di una piccola dimensione familiare milanese.
Ringrazio i miei colleghi di magistrale: **Claudia**, la mia amica del cuore milano-calabrese, con la quale ho condiviso praticamente l'intero percorso di vita milanese, sia all'interno che all'esterno dell'universitá, **Antonella**, una persona meravigliosa da ogni punto di vista,

tremendamente sensivbile ed empatica, che ho avuto la fortuna di conoscere il primo giorno di lezioni e non mollare piú, **Livia**, che è stata la mia guida pratica fin dal primo giorno al Politecnico, sempre spontanea e disponibile, **Veronica**, che è allo stesso tempo un'amica dolcissima ed una folle compagna di avventure,**Ilaria**, un'amica dalla solaritá coinvolgente, **Ludovica**, compagna di ansie, con la quale ho avuto il piacere dei piú bei scambi musicali, **Federica**, la persona piú buona dell'universo, la tua ironia mi tira sempre su di morale, **Giovanni**, l'intellettuale bohemién, che mi insegna a preoccuparmi meno dei mali della vita, e **Lorenzo**, la cui gentilezza mi spiazza.
Ringrazio **Alessandro**, che mi ha sempre motivato e tirato su di morale nei momenti piú bui, seppur dalla lontana Francia.
Infine ringrazio **Omar**, sebbene tu sia entrato nella mia vita da poco, mi hai supportato nel momento per me piú difficile, donandomi gioia e spensieratezza. Sappi che sono felice.